

Fig. 3 Temporal pattern of differential gene expression in spinal cords. The expression of indicated genes were detected by the RT-PCR analysis in 7-, 11-, 14- and 17-week-old mutant SOD1 and normal littermate mice. Quantitation of mRNA levels is given as a ratio of intensity of mutant SOD1 against littermate mice, after adjusting those to β -actin levels. The values plotted are the means of the duplicate experiments in each group consisting of between three and five pooled spinal cords.

signaling, was also induced in 11-week-old mutant SOD1 mice. Histopathological evaluation showed glial cell activation and proliferation as early as 11 weeks of age, and continuing to advance until 17 weeks of age (Hall *et al.* 1998), which is consistent with the temporal gene expression pattern of the inflammatory process-related genes mentioned above. These results indicate that an inflammation was not simply a reaction to massive neuron death as motor neuron loss in spinal cords began to occur around 14 weeks of age at comparable levels. In particular, TNF- α produced by activated microglia, which is a proinflammatory cytokine having both neurotoxic and neuroprotective effects (Terrado *et al.* 2000), was greatly elevated in its gene expression even in 11-week-old mutant SOD1 mice. It has been reported that TNF- α protein was increased in the blood of patients with

ALS (Poloni *et al.* 2000), and mRNA levels of TNF- α and interleukin-1 β (IL-1 β) were elevated in spinal cord of wobbler mice, which is another model of human ALS (Schlomann *et al.* 2000). We also noted that spinal motor neurons expressed TNF- α and cathepsin D of the lysosomal system, which might implicate neuron–glial interactions during the inflammatory process of neurodegeneration. In the symptomatic stage, the change of gene expression of clusterin in the complement system was associated with the inflammation. Taken together, these results suggest that the inflammatory components play an instrumental role in neurodegeneration in spinal cords of mutant SOD1 mice.

In mutant SOD1 mice, caspase-1 localized in spinal motor neurons was activated earliest, 3 weeks prior to motor neuron death, as reported by other investigators (Li *et al.* 2000;

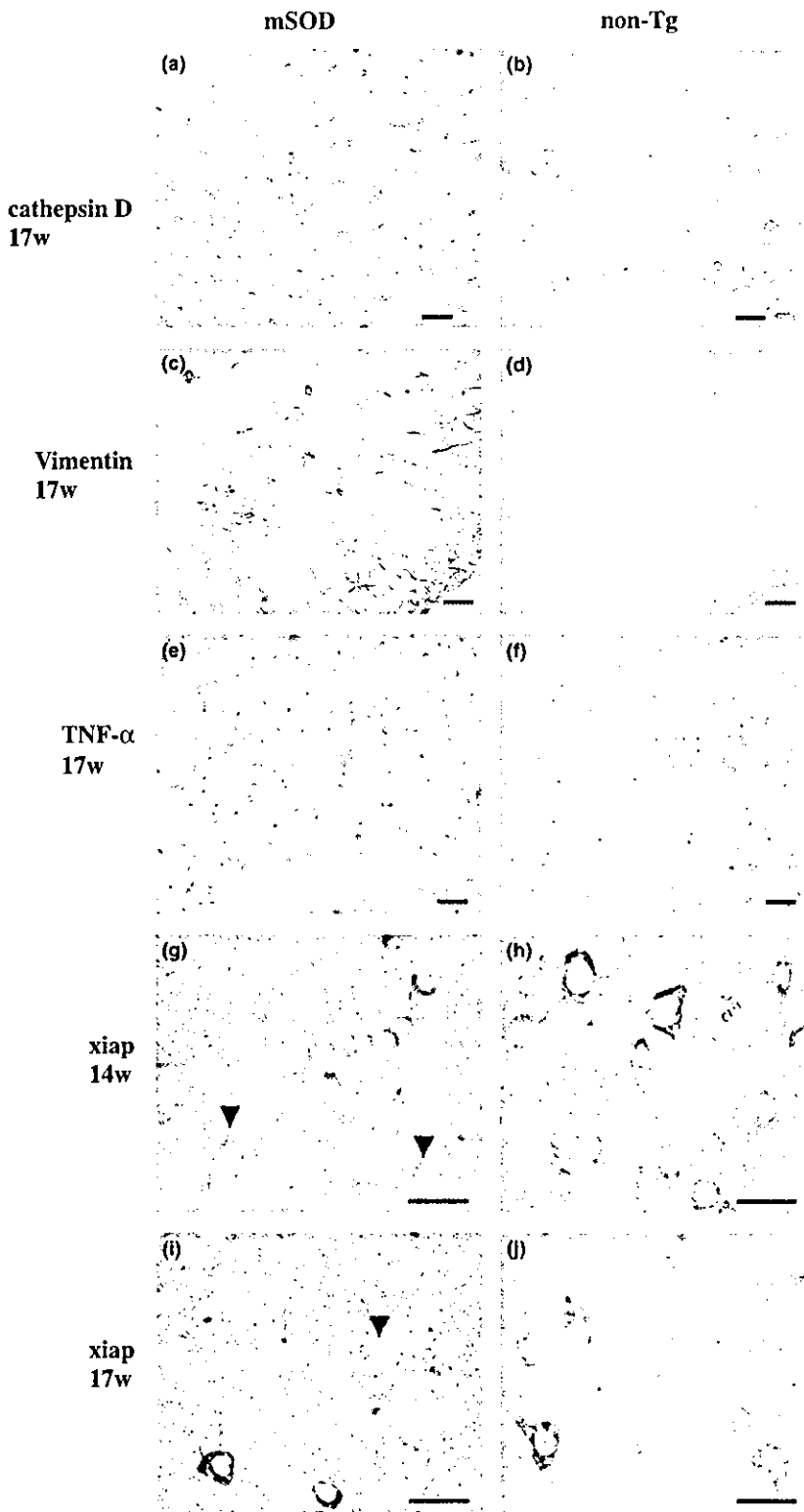


Fig. 4 *In situ* localization of differential gene expression in spinal cords. Representative photomicrographs show the changes in the cathepsin D, vimentin and TNF- α immunoreactivities at 17 weeks of age in the spinal cord of mutant SOD1 transgenic (mSOD) mice (a, c and e), compared with non-transgenic (non-Tg) control mice (b, d and f). Cathepsin D immunoreactivity was observed in motor neurons in non-transgenic littermates (b), while in mutant SOD mice (a) its expression was elevated in glial cells. Strong vimentin immunoreactivity is demonstrated in glial cells in mutant SOD1 mice (c), but it was not detectable in control mice (d). TNF- α immunoreactivity was clearly detectable in microglia and motor neurons in mutant SOD1 mice (e) in contrast with weak TNF- α labeling in littermate mice (f). In mutant SOD1 mice, the xiap signals of *in situ* hybridization were significantly decreased in motor neurons (arrowheads) as well as in glial cells at 14 (g) and 17 weeks (i) of age, compared with those in non-transgenic mice (h and j). Controls for specificity of immunostaining included omission of the primary antibody, preincubation of the antibody with the immunogen and incubation of sections with non-immune rabbit or rat sera. *In situ* hybridization after RNase treatment, without antisense probe or anti-digoxigenin antibody abolished positive signals and served as a negative control, together with hybridization with sense probe. Scale bar: (a), (b), (e), (f), (g), (h), (i) and (j), 50 μ m; (c) and (d), 100 μ m.

Pasinelli *et al.* 2000). We demonstrated that the gene expression of TNF- α and CD68 was up-regulated together with caspase-1 at 11 weeks of age in mutant SOD1 mice. In addition to the role of an initiator of the neuronal apoptotic

cascade, extracellular caspase-1 converts IL-1 β into mature form. Thus, caspase-1 activation in motor neurons contributes to an inflammatory pathway with early astrocytosis and microglial activation in mutant SOD1 mice. A key

Table 2 Ratio of gene expressions using microarray analysis

Genes	GenBank accession number	Expression ratio	
		11w	17w
vimentin	X51438	1.6	8.6
TNF- α	M38296	5.3*	8.0*
snail protein homolog (SNAI1)	M95604	0.9	6.3
prothymosin β 4	X16053	1.0	5.4
WNT7A	M89801	2.0	5.3
clusterin precursor	L08235	1.1	5.3
c-fos proto-oncogene	V00727	1.2	4.9
developing brain homeobox protein	S75837	1.6	4.2
P-selectin glycoprotein ligand 1	X91144	1.0	4.2
CD147	D00611	1.4	4.0
low-density lipoprotein receptor	Z19521	2.2	3.7
Janus tyrosine-protein kinase 3 (JAK3)	L33768	2.0	3.7
junD1, jun proto-oncogene-related gene	J05205	1.2	3.6
cathepsin D (CTSD)	X53337	1.4	3.5
BCL2-like protein 1 (BCL2L1), Bcl-xL	L35049	1.0	3.5
Tiam-1 invasion inducing protein	U05245	1.3	3.5
CD68	NM_009853	2.3*	3.5*
preproenkephalin 2 (PENK2)	M55181	1.7	3.4
serine protease inhibitor 2-2	M64086	1.0	3.4
cystatin C precursor	M59470	1.0	3.4
sine oculis-related homeobox protein homolog (SIX2)	X80338	0.8	3.3
α -internexin neuronal intermediate filament protein	L27220	1.5	3.3
CD7 antigen	D10329	1.3	3.3
serine protease inhibitor 2-4	X69832	1.4	3.2
linker for activation of T-cells (LAT)	AF036907	1.4	3.2
kinesin motor protein 3C (KIF3C)	AF013116	2.1	3.2
retinoid X receptor- α	M84817	2.2	3.2
platelet-derived growth factor A	M29464	1.4	3.1
genomic screened homeobox protein 2 (GSH2)	S79041	1.0	3.1
GFAP	K01347	1.8*	3.1*
CREB-binding protein	S66385	1.1	3.0
gastrulation brain homeobox 2 (GBX2)	L39770	2.2	3.0
SHC-transforming protein	U15784	1.5	3.0
caspase-1	L28095	2.8*	3.0*
mIAP3, xiap	U88990	1.0	0.3
otogelin (OTOG)	U96411	1.6	0.3
Rab GDP-dissociation inhibitor- α ; GDI-1	U07950	1.0	0.3
calbindin 2	X73985	2.0	0.3
fibroblast growth factor 6 precursor	M92415	2.9	0.3
transducin-like enhancer of split protein 3	X73360	1.7	0.1
GABA _A receptor α 1	M86566	1.0	0.1

The expression ratio was calculated by dividing fluorescence intensity of gene elements in mSOD mice by fluorescence intensity of gene elements in control mice. *Genes calculated by RT-PCR analysis.

executioner of apoptosis, caspase-3, resulting from caspase-1 activation, began to be up-regulated at 14 weeks of age (Li *et al.* 2000). This finding agrees with the present result that at 14 weeks of age xiap mRNA down-regulation occurred in the spinal cords of mutant SOD1 mice since Xiap is a direct inhibitor of caspase-3, -7 and -9 (Deveraux *et al.* 1997; Datta *et al.* 2000). Neuronal apoptosis has been shown to underlie

several neurodegenerative diseases including Alzheimer's disease (Lassmann *et al.* 1995; Stadelmann *et al.* 1999), prion diseases (Gray *et al.* 1999) and HIV-dementia (Gray *et al.* 2000). In these reports, there is strong evidence for an inflammatory response involving microglial activation that leads to neuronal apoptosis. Activated microglia express neurotoxic cytokines and substances, such as TNF- α ,

proteases, oxyradicals and small reactive molecules (Minghetti and Levi 1998). The lines of evidence validate an interrelationship between the inflammatory reaction and apoptotic pathway, both of which participate in the relentless neurodegenerative process, making for a detrimental cycle.

The transcripts that were highly up-regulated in spinal cords of mutant SOD1 mice include those related to the differentiation and maturation of the spinal cord cell population. Retinoic acid is known to be an inducer of neuronal differentiation. The increased expression of retinoid X receptor α from the early symptomatic stage may be a compensatory response for motor neuron degeneration. The importance of retinoid signaling in motor neuronal differentiation in spinal cord has been clearly demonstrated (Sockanathan and Jessell 1998). Moreover, homeobox proteins, which are transcription factors for the differentiation and maturation of motor neurons in the spinal cord originating from multipotent neural stem cells in the neural tube, were up-regulated in expression levels in mutant SOD1 mice. These results imply a potential involvement of the differentiation signals in maintaining motor neuron integrity with great interest, which might be impaired in the neurodegenerative process of mutant SOD1.

We detected the significant up-regulation of 34 specific transcripts and down-regulation of seven transcripts in the spinal cords of mutant SOD1 mice. These include genes known to be involved in the inflammatory and anti-apoptotic cascades, comprising proinflammatory cytokines, cathepsin and caspase proteases. The expression of cyclooxygenase type-2 (Cox-2), a key enzyme in the synthesis of prostanoïd, has been reported to increase in early symptomatic mutant SOD1 mice (Almer *et al.* 2001). Although the up-regulation of the protease inhibitors, such as cystatin C of cathepsin protease inhibitors, and serine protease inhibitors occurred intrinsically, these inhibitors cannot rescue spinal motor neurons from degenerative and death processes. The sufficient and early inhibition of the inflammatory process, using the inhibitors for protease, Cox-2 and TNF- α , may be a valuable therapeutic avenue for the amelioration of FALS and possibly other neurodegenerative disorders. The simultaneous blocking of the apoptotic cascade by caspase inhibitors, which would result in anti-inflammatory effects based on the interaction of inflammation and apoptosis, could help to hamper the disease progression.

In conclusion, the present study identified alterations in the expression levels of numerous transcripts in spinal cords of mutant SOD1 mice compared with comparable data obtained from normal littermates, employing large-scale and custom cDNA microarrays. Recently, Malaspina *et al.* (2001) have reported up-regulation of transcripts involved in neuro-inflammatory cascades in human ALS spinal cords using gridded microarrays, being consistent with our findings. We speculate that the differential changes of inflammation- and apoptosis-related gene expression reflect the mechanism of

neurodegeneration during the onset and progression of FALS. To develop a new therapeutic strategy against inflammatory and apoptotic cascades, the expression profiles specific to individual spinal motor neurons and glial cells in particular, remain to be elucidated.

Acknowledgements

This work was supported by a grant for Center of Excellence (COE) from the Ministry of Education, Culture, Sports, Science and Technology of Japan.

References

- Almer G., Guegan C., Teismann P., Naini A., Rosoklija A., Hays A. P., Chen C. C. and Przedborski S. (2001) Increased expression of the pro-inflammatory enzyme, cyclooxygenase-2 in amyotrophic lateral sclerosis. *Ann. Neurol.* **49**, 176–185.
- Beal M. F., Ferrante R. J., Browne S. E., Matthews R. T., Kowall N. W. and Brown R. H. Jr (1997) Increased 3-nitrotyrosine in both sporadic and familial amyotrophic lateral sclerosis. *Ann. Neurol.* **42**, 644–654.
- Bitsch A., da Costa C., Bunkowski S., Weber F., Rieckmann P. and Bruck W. (1998) Identification of macrophage populations expressing tumor necrosis factor- α mRNA in acute multiple sclerosis. *Acta Neuropathol.* **95**, 373–377.
- Brown R. H. Jr (1995) Amyotrophic lateral sclerosis: recent insights from genetics and transgenic mice. *Cell* **80**, 687–692.
- Cudkovicz M. E., McKenna-Yasek D., Sapp P. E., Chin W., Geller B., Hayden D. L., Schoenfeld D. A., Hosler B. A., Horvitz H. R. and Brown R. H. (1997) Epidemiology of mutations in superoxide dismutase in amyotrophic lateral sclerosis. *Ann. Neurol.* **41**, 210–221.
- Cui J., Holmes E. H. and Liu P. K. (1999) Oxidative damage to the c-fos gene and reduction of its transcription after focal cerebral ischemia. *J. Neurochem.* **73**, 1164–1174.
- Datta R., Oki E., Endo K., Biedermann V., Ren J. and Kufe D. (2000) XIAP regulates DNA damage-induced apoptosis downstream of caspase-9 cleavage. *J. Biol. Chem.* **275**, 31733–31738.
- Deveraux Q. L., Takahashi R., Salvesen G. S. and Reed J. C. (1997) X-linked IAP is a direct inhibitor of cell-death proteases. *Nature* **388**, 300–304.
- Engler-Blum G., Meier M., Frank J. and Muller G. A. (1993) Reduction of background problems in nonradioactive northern and southern blot analyses enables higher sensitivity than ^{32}P -based hybridizations. *Anal. Biochem.* **210**, 235–244.
- Ferrante R. J., Browne S. E., Shinobu L. A., Bowling A. C., Baik M. J., MacGarvey U., Kowall N. W., Brown R. H. Jr and Beal M. F. (1997) Evidence of increased oxidative damage in both sporadic and familial amyotrophic lateral sclerosis. *J. Neurochem.* **69**, 2064–2074.
- Friedman L. K., Belayev L., Alfonso O. F. and Ginsberg M. D. (2000) Distribution of glutamate and preproenkephalin messenger RNAs following transient focal cerebral ischemia. *Neuroscience* **95**, 841–857.
- Gray F., Chretien F., Adle-Biassette H., Dorandeu A., Ereau T., Delisle M. B., Kopp N., Ironside J. W. and Vital C. (1999) Neuronal apoptosis in Creutzfeldt–Jakob disease. *J. Neuropathol. Exp. Neurol.* **58**, 321–328.
- Gray F., Adle-Biassette H., Brion F., Ereau T., Le Maner I., Levy V. and Crochet G. (2000) Neuronal apoptosis in human immunodeficiency virus infection. *J. Neurovirol.* **6**, S38–S43.

- Gurney M. E., Pu H., Chiu A. Y., Dal Canto M. C., Polchow C. Y., Alexander D. D., Caliendo J., Hentati A., Kwon Y. W., Deng H. X., Chen W., Zhai P., Sufit R. L. and Siddique T. (1994) Motor neuron degeneration in mice that express a human Cu, Zn superoxide dismutase mutation. *Science* **264**, 1772–1775.
- Hall E. D., Oostveen J. A. and Gurney M. E. (1998) Relationship of microglial and astrocytic activation to disease onset and progression in a transgenic model of familial ALS. *Glia* **23**, 249–256.
- Haverkamp L. I., Appel V. and Appel S. H. (1995) Natural history of amyotrophic lateral sclerosis in a database population: validation of a scoring system and a model for survival prediction. *Brain* **118**, 707–719.
- Hill S. J., Barbarese E. and McIntosh T. K. (1996) Regional heterogeneity in the response of astrocytes following traumatic brain injury in the adult rat. *J. Neuropathol. Exp. Neurol.* **55**, 1221–1229.
- Inoue H., Sawada M., Ryo A., Tanahashi H., Wakatsuki T., Hada A., Kondoh N., Nakagaki K., Takahashi K., Suzumura A., Yamamoto M. and Tabira T. (1999) Serial analysis of gene expression in a microglial cell line. *Glia* **28**, 265–271.
- Ishigaki S., Niwa J., Yoshihara T., Mitsuma N., Doyu M. and Sobue G. (2000) Two novel genes, human *neugrin* and mouse *m-neugrin*, are upregulated with neuronal differentiation in neuroblastoma cells. *Biochem. Biophys. Res. Commun.* **279**, 526–533.
- Kamme F. and Wieloch T. (1996) Induction of junD mRNA after transient forebrain ischemia in the rat. Effect of hypothermia. *Brain Res. Mol. Brain Res.* **43**, 51–56.
- Lassmann H., Bancher C., Breitschopf H., Wegiel J., Bobinski M., Jellinger K. and Wisniewski H. M. (1995) Cell death in Alzheimer's disease evaluated by DNA fragmentation *in situ*. *Acta Neuropathol.* **89**, 35–41.
- Li M., Ona V. O., Guegan C., Chen M., Jackson-Lewis V., Andrews L. J., Olszewski A. J., Stieg P. E., Lee J.-P., Przedborski S. and Friedlander R. M. (2000) Functional role of caspase-1 and caspase-3 in an ALS transgenic mouse model. *Science* **288**, 335–339.
- Lu J., Mochhala S., Kaur C. and Ling E. (2000) Changes in apoptosis-related protein (p53, Bax, Bcl-2 and Fos) expression with DNA fragmentation in the central nervous system in rats after closed head injury. *Neurosci. Lett.* **290**, 89–92.
- Malaspina A., Kaushik N. and De Bellerocche J. (2001) Differential expression of 14 genes in amyotrophic lateral sclerosis spinal cord detected using gridded cDNA arrays. *J. Neurochem.* **77**, 132–145.
- Minghetti L. and Levi G. (1998) Microglia as effector cells in brain damage and repair. Focus on prostanoids and nitric oxide. *Prog. Neurobiol.* **54**, 99–125.
- Mitsuma N., Yamamoto M., Li M., Ito Y., Mitsuma T., Mutoh T., Takahashi M., Sobue G. (1999) Expression of GDNF receptor (RET and GDNFR- α) mRNAs in the spinal cord of patients with amyotrophic lateral sclerosis. *Brain Res.* **820**, 77–85.
- Mitsumoto H. (1997) Diagnosis and progression of ALS. *Neurology* **48**, 2–8.
- Palm D. E., Knuckey N. W., Primiano M. J., Spangenberg A. G. and Johanson C. E. (1995) Cystatin C, a protease inhibitor, in degenerating rat hippocampal neurons following transient forebrain ischemia. *Brain Res.* **691**, 1–8.
- Pasinelli P., Houseweart M. K., Brown R. H. Jr and Cleveland D. W. (2000) Caspase-1 and -3 are sequentially activated in motor neuron death in Cu, Zn superoxide dismutase-mediated familial amyotrophic lateral sclerosis. *Proc. Natl Acad. Sci. USA* **97**, 13901–13906.
- Pedersen W. A., Fu W., Keller J. N., Markesbery W. R., Appel S. A., Smith R. G., Kasarkis E. and Mattson M. P. (1998) Protein modification by the lipid peroxidation product 4-hydroxynonenal in the spinal cords of amyotrophic lateral sclerosis patients. *Ann. Neurol.* **44**, 819–824.
- Poloni M., Facchetti D., Mai R., Micheli A., Agnoletti L., Francolini G., Mora G., Camana C., Mazzini L. and Bachetti T. (2000) Circulating levels of tumour necrosis factor- α and its soluble receptors are increased in the blood of patients with amyotrophic lateral sclerosis. *Neurosci. Lett.* **287**, 211–214.
- Reaume A. G., Elliott J. L., Hoffman E. K., Kowall N. W., Ferrante R. J., Siwek D. F., Wilcox H. M., Flood D. G., Beal M. F., Brown R. H., Scott R. W. and Snider W. D. (1996) Motor neurons in Cu/Zn superoxide dismutase-deficient mice develop normally but exhibit enhanced cell death after axonal injury. *Nat. Genet.* **13**, 43–47.
- Schlomann U., Rathke-Hartlieb S., Yamamoto S., Jockusch H. and Bartsch J. W. (2000) Tumor necrosis factor alpha induces a metalloprotease-disintegrin, ADAM8 (CD 156); implications for neuron–glia interactions during neurodegeneration. *J. Neurosci.* **20**, 7964–7971.
- Sockanathan S. and Jessell T. M. (1998) Motor neuron-derived retinoid signaling specifies the subtype identity of spinal motor neurons. *Cell* **94**, 503–514.
- Stadelmann C., Deckwerth T. L., Srinivasan A., Bancher C., Bruck W., Jellinger K. and Lassmann H. (1999) Activation of caspase-3 in single neurons and autophagic granules of granulovacuolar degeneration in Alzheimer's disease. Evidence for apoptotic cell death. *Am. J. Pathol.* **155**, 1459–1466.
- Terrado J., Monnier D., Perrelet D., Vesin D., Jemelin S., Buurman W. A., Mattenberger L., King B., Kato A. C. and Garcia I. (2000) Soluble TNF receptors partially protect injured motoneurons in the postnatal CNS. *Eur. J. Neurosci.* **12**, 3443–3447.
- Tu P. H., Raju P., Robinson K. A., Gurney M. E., Trojanowski J. Q. and Lee V. M. (1996) Transgenic mice carrying a human mutant superoxide dismutase transgene develop neuronal cytoskeletal pathology resembling human amyotrophic lateral sclerosis lesions. *Proc. Natl Acad. Sci. USA* **93**, 3155–3160.
- Vartiainen N., Pyykonen I., Hokfelt T. and Koistinaho J. (1996) Induction of thymosin beta(4) mRNA following focal brain ischemia. *Neuroreport* **7**, 1613–1616.
- Wong P. C., Pardo C. A., Borchelt D. R., Lee M. K., Copeland N. G., Jenkins N. A., Sisodia S. S., Cleveland D. W. and Price D. L. (1995) An adverse property of a familial ALS-linked SOD1 mutation causes motor neuron disease characterized by vacuolar degeneration of mitochondria. *Neuron* **14**, 1105–1116.
- Yamamoto M., Li M., Mitsuma N., Ito S., Kato M., Takahashi M. and Sobue G. (2001) Preserved phosphorylation of RET receptor protein in spinal motor neurons of patients with amyotrophic lateral sclerosis: an immunohistochemical study by a phosphorylation-specific antibody at tyrosine 1062. *Brain Res.* **912**, 89–94.
- Yim M. B., Kang J. H., Yim H. S., Kwak H. S., Chock P. B. and Stadman E. R. (1996) A gain-of-function of an amyotrophic lateral sclerosis-associated Cu,Zn-superoxide dismutase mutant. An enhancement of free radical formation due to a decrease in K_m for hydrogen peroxide. *Proc. Natl Acad. Sci. USA* **93**, 5709–5714.

Dorfin Ubiquitylates Mutant SOD1 and Prevents Mutant SOD1-mediated Neurotoxicity*

Received for publication, July 2, 2002
Published, JBC Papers in Press, July 26, 2002, DOI 10.1074/jbc.M206559200

Jun-ichi Niwa^{‡§}, Shinsuke Ishigaki[‡], Nozomi Hishikawa[‡], Masahiko Yamamoto[‡], Manabu Doyu[‡], Shigeo Murata[¶], Keiji Tanaka[¶], Naoyuki Taniguchi[¶], and Gen Sobue^{‡**}

From the [‡]Department of Neurology, Nagoya University Graduate School of Medicine, Showa-ku, Nagoya 466-8550, Japan, the [¶]Department of Molecular Oncology, Tokyo Metropolitan Institute of Medical Science, Bunkyo-ku, Tokyo 113-8613, Japan, and the [§]Department of Biochemistry, Osaka University Graduate School of Medicine, Suita, Osaka 565-0871, Japan

Amyotrophic lateral sclerosis (ALS) is a progressive paralytic disorder resulting from the degeneration of motor neurons in the cerebral cortex, brainstem, and spinal cord. The cytopathological hallmark in the remaining motor neurons of ALS is the presence of ubiquitylated inclusions consisting of insoluble protein aggregates. In this paper we report that Dorfin, a RING finger-type E3 ubiquitin ligase, is predominantly localized in the inclusion bodies of familial ALS with a copper/zinc superoxide dismutase (SOD1) mutation as well as sporadic ALS. Dorfin physically bound and ubiquitylated various SOD1 mutants derived from familial ALS patients and enhanced their degradation, but it had no effect on the stability of the wild-type SOD1. The overexpression of Dorfin protected against the toxic effects of mutant SOD1 on neural cells and reduced SOD1 inclusions. Our results indicate that Dorfin protects neurons by recognizing and then ubiquitylating mutant SOD1 proteins followed by targeting them for proteasomal degradation.

Amyotrophic lateral sclerosis (ALS)¹ is a neurodegenerative disease characterized by the loss of motor neurons in the cerebral cortex, brain stem, and spinal cord (1, 2). Although most patients with ALS are sporadic cases, 5–10% of ALS patients show a familial trait, and in 10–20% of these patients this trait is associated with mutations in the *SOD1* gene (3). Although many scenarios for understanding ALS pathogenesis have been proposed (4–6), to date the exact mechanisms causing the disease are still unknown. In considering the pathogenesis of

ALS, it is important that the inclusion bodies, which consist of aggregated, ubiquitylated proteins surrounded by disorganized filaments, are frequently seen in the surviving motor neurons in both sporadic and familial ALS (7–12). Interestingly, SOD1 is reported to be the major component of the neuronal hyaline inclusion (NHI) of familial ALS associated with SOD1 mutation (13). In addition, the NHI in the motor neurons of familial ALS is commonly stained with anti-ubiquitin (Ub)-antibody, but it remains uncertain whether SOD1 itself is ubiquitylated with respect to the inclusion body formation. To clarify the mechanisms underlying the inclusion body formation and consequent motor neuron degeneration in ALS, it is important to know how SOD1 and/or other protein component(s) are ubiquitylated.

Dorfin is a gene product we cloned from the anterior horn tissues of the human spinal cord (14). Dorfin contains two RING finger motifs and an in-between RING finger (IBR) domain at the N terminus (14). The RING finger/IBR motif was identified in several protein sequences through a data base search (15). It was reported that HHARI (human homologue of ariadne) and H7-AP1 (UbcH7-associated protein), which are both RING finger/IBR motif-containing proteins, interact with the ubiquitin-conjugating enzyme (E2) UbcH7 through the RING finger/IBR motif and that a distinct subclass of RING finger/IBR motif-containing proteins represents a new family of proteins that specifically interact with distinct E2 enzymes (16, 17). Parkin, a gene product responsible for one of the most common forms of the familial Parkinson's disease (PD) (18), has a RING finger/IBR motif, binds with UbcH7 and UbcH8, and has ubiquitin-protein ligase (E3) activities (19–21). Several proteins with RING finger motifs have been characterized as E3 ubiquitin ligases (22–24). In RING-type E3s, the RING finger motifs function as recruiting motifs for specific E2s (25–28). These facts suggest that RING finger/IBR family proteins are new members of the RING-type E3 family. We found that Dorfin interacts with UbcH7 or UbcH8 through the RING finger/IBR domain and mediates E3 activity (14).

We reported previously (14) that Dorfin is mainly localized in the centrosomal region and forms an aggresome-like structure. Aggresomes are pericentriolar cytoplasmic inclusions containing misfolded ubiquitylated proteins, which appear when the cell fails to further degrade misfolded proteins (29). In addition, cultured cells expressing mutant SOD1 have been demonstrated to form an aggresome-like structure (30). Based on this background, we postulated that Dorfin could be critically important in the formation of ubiquitylated inclusion bodies in ALS. We show here that Dorfin is localized in the inclusion bodies found in the motor neurons of familial ALS with a SOD1 mutation as well as sporadic ALS and mutant SOD1-trans-

* This work was supported in part by a Center of Excellence (COE) grant from the Ministry of Education, Culture, Sports, Science and Technology and grants from the Ministry of Health, Labor and Welfare of Japan. The costs of publication of this article were defrayed in part by the payment of page charges. This article must therefore be hereby marked "advertisement" in accordance with 18 U.S.C. Section 1734 solely to indicate this fact.

§ Research fellow of the Japan Society for the Promotion of Science for Young Scientists.

** To whom correspondence should be addressed: Department of Neurology, Nagoya University Graduate School of Medicine, 65 Tsurumai-cho Showa-ku, Nagoya 466-8550, Japan. Tel.: 81-52-744-2385; Fax: 81-52-744-2384; E-mail: sobueg@med.nagoya-u.ac.jp.

¹ The abbreviations used are: ALS, amyotrophic lateral sclerosis; SOD1, copper/zinc superoxide dismutase; NHI, neuronal hyaline inclusion; Ub, ubiquitin; IBR, in-between RING finger; HEK293, human embryonic kidney 293; E2, ubiquitin-conjugating enzyme; E3, ubiquitin-protein ligase; IP, immunopurified; PI, propidium iodide; GFP, green fluorescent protein; MTT, 3-(4,5-dimethylthiazol-2-yl)-2,5-diphenyltetrazolium bromide; PD, Parkinson's disease; CHIP, carboxyl terminus of Hsc70-interacting protein; Hsp, heat shock protein.

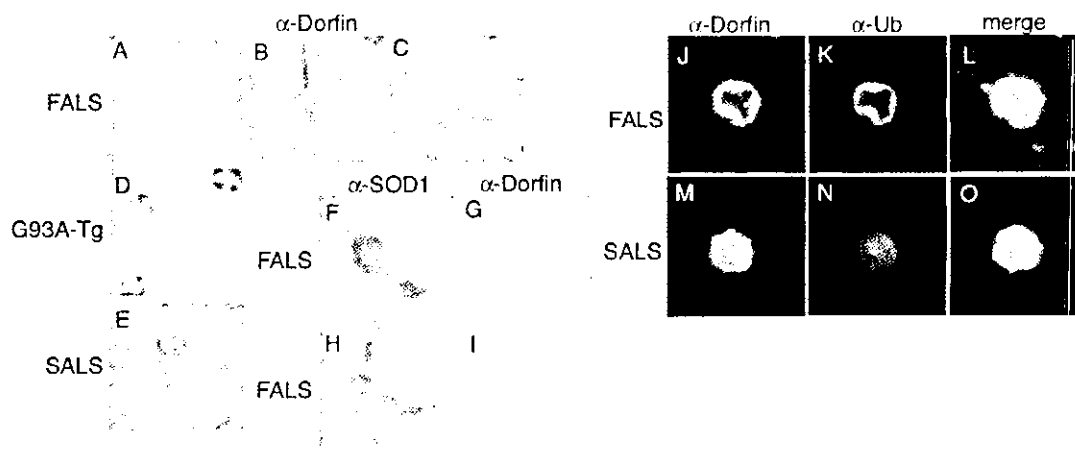


FIG. 1. Localization of Dorfin in inclusion bodies in spinal cord motor neurons of ALS and mutant SOD1-transgenic mice. The transverse sections of the spinal cord from familial ALS (FALS; panels A–C), SOD1^{G93A}-transgenic mice (G93A-Tg, panel D), and sporadic ALS (SALS, panel E) were immunohistochemically stained with the anti-Dorfin antibody. The hyaline inclusions in familial ALS were stained with anti-SOD1 (α -SOD1, panels F and H) or anti-Dorfin (α -Dorfin, panels G and I) antibodies. Note that panels F and G or H and I are the identical sections doubly immunostained. Spinal cord sections from familial (panels J–L) and sporadic (panels M–O) ALS were double labeled by indirect immunofluorescence with anti-Dorfin antibody (panels J and M) and monoclonal antibody to Ub (α -Ub, panels K and N) and observed by a laser-scanning confocal microscope. Panel L is panels J and K merged; panel O is panels M and N merged. Magnification, $\times 225$ (panels A–C, E and F–I) and $\times 675$ (panels D and J–O).

genic mice and is involved in the ubiquitylation and targeted degradation of mutant SOD1.

EXPERIMENTAL PROCEDURES

Immunohistochemistry—Immunohistochemical studies were carried out on 10% formalin-fixed, paraffin-embedded spinal cords filed in the Department of Neurology, Nagoya University Graduate School of Medicine. The specimens were obtained at autopsy from two familial ALS patients with mutant SOD1^{N86S} (male aged 57 years and female aged 54 years), three sporadic cases of ALS (all males, aged 46, 59, and 67 years) and four age-matched, non-neurologic disease patients. The spinal cord specimens of these ALS cases and those of mutant SOD1^{G93A}-transgenic mice (B6SJL-Tg(SOD1-G93A)1Gur; The Jackson Laboratory) were immunohistochemically stained with antibodies against Dorfin (14), SOD1 (SOD-100; StressGen Biotechnologies, La Jolla, CA), and Ub (P4D1; Santa Cruz Biotechnology). Double staining of identical sections was performed as described (31). In immunofluorescence microscopy, Alexa-488- and Alexa-546-conjugated secondary antibodies (Molecular Probes) were used. The human and animal studies described in this report were approved by the Ethics Review Committees of the Nagoya University Graduate School of Medicine.

Expression Plasmids, Cell Culture, and Transfection—Human wild-type SOD1 and mutant SOD1^{G37R}, SOD1^{H46R}, SOD1^{G85R}, and SOD1^{G93A} cDNAs containing the entire coding region were inserted in-frame into the *Bam*HI and *Xho*I site of pcDNA3.1(+)/MycHis vector (Invitrogen) or into the *Xho*I and *Bam*HI site of the pEGFP-N1 vector (CLONTECH). Construction of a pcDNA3.1(+)/FLAG-Ub vector and the Dorfin or Dorfin deletion mutant (Dorfin-N and Dorfin-C) pcDNA4/HisMax vectors was reported elsewhere (14). Human embryonic kidney 293 (HEK293) cells and Neuro2a cells were maintained in Dulbecco's modified Eagle's medium with 10% fetal calf serum. Transfections were performed using the Effectene transfection reagent (Qiagen). Cells were lysed in lysis buffer (50 mM Tris, 150 mM NaCl, 1% Nonidet P-40, and 0.1% SDS) with a protease inhibitor mixture. To inhibit cellular proteasome activity, cells were treated with 0.5 μ M MG132 (*N*-benzyloxycarbonyl-Leu-Leu-leucinal; Sigma) for 16 h after overnight post-transfection.

In Vitro Ubiquitylation Assay and Pulse-Chase Analysis—Immunopurified (IP) Xpress-Dorfin bound to anti-Xpress antibody (Invitrogen) with protein G beads (Amersham Biosciences) was prepared from lysates of HEK293 cells transfected with 1.5 μ g of pcDNA4/HisMax-Dorfin or Dorfin deletion mutants. IP-SOD1-Myc was prepared with anti-Myc IgG-linked protein A beads (Santa Cruz Biotechnology) from lysates of HEK293 cells transfected with 1 μ g of pcDNA3.1(+)/MycHis wild-type or mutant SOD1. Slurries of IP-Xpress-Dorfin were mixed with IP-Myc-SOD1 and incubated at 30 $^{\circ}$ C for 90 min in 50 μ l of reaction buffer containing ATP (4 mM ATP in 50 mM Tris-HCl, pH 7.5, and 2 mM MgCl₂), 100 ng of rabbit E1 (Calbiochem), 2 μ M of UbcH7 (Affiniti, Exeter, United Kingdom), and 2 μ g of His-Ub (Calbiochem). The reaction was terminated by adding 20 μ l of 4 \times sample buffer, and 20- μ l aliquots of the reaction mixtures were subjected to SDS-

PAGE followed by Western blotting. Pulse-chase analysis of SOD1-transfected HEK293 cells was performed as described previously (30). Pulse labeling was performed with 250 μ Ci/ml [³⁵S]Cys for 45 min. After washing in phosphate-buffered saline (PBS), the cells were chased for the indicated time intervals in complete medium. Samples were immunoprecipitated with anti-Myc antibody, separated on 5–20% SDS/PAGE, and analyzed by phosphorimaging (BAS2000; Fujix, Tokyo, Japan).

Neurotoxicity Analysis and Quantification of SOD1 Aggregates— 4×10^4 Neuro2a cells were grown overnight on 2-well collagen-coated slides. They were transfected with 0.4 μ g of pcDNA3.1(+)/MycHis-SOD1, 0.4 μ g of pcDNA4/HisMax-Dorfin, and 0.4 μ g of pEGFP-C3 vector (CLONTECH). pcDNA4/HisMax-LacZ was used as control instead of Dorfin. Cells were incubated for 16 h, and the medium was then replaced with serum-free medium. Cell death was determined in propidium iodide (PI)-stained preparations at 48 h after serum deprivation. The ratio of dead cells was expressed as the percentage of PI- and GFP-positive cells in GFP-positive cells. For cell viability assay, 5×10^3 Neuro2a cells were grown in 96-well collagen-coated plates overnight. They were then transfected with 0.1 μ g of pcDNA3.1(+)/MycHis-SOD1 and 0.1 μ g of pcDNA4/HisMax-Dorfin. pcDNA4/HisMax-LacZ was used as control instead of Dorfin. The 3-(4,5-dimethylthiazol-2-yl)-2,5-diphenyltetrazolium bromide (MTT)-based cell proliferation assay was then performed using CellTiter 96 (Promega) at 0, 24, and 48 h after incubation. The assay was carried out in triplicate. Absorbance at 490 nm was measured in a multiple plate reader. For quantification of SOD1 aggregates, Neuro2a cells transfected with pEGFP-N1-SOD1 and pcDNA4/HisMax-Dorfin or -LacZ were examined using a confocal microscope (Radiance; Bio-Rad). All cells were counted in fields selected at random from four different quadrants of the culture well. Counting was performed by an investigator blind to the experimental condition.

RESULTS

Dorfin Is Localized in the Inclusion Bodies in ALS Motor Neuron—Immunohistochemical analysis revealed that Dorfin was predominantly localized in the NHI found in familial ALS (Fig. 1, A–C) and mutant SOD1^{G93A}-transgenic mice (Fig. 1D) as well as in sporadic ALS (Fig. 1E). About 50% of NHIs were positively stained for Dorfin. Dorfin immunoreactivity was concentrated either at the periphery of the inclusion (Fig. 1A) or throughout it (Fig. 1B). Some aggregates localized in neuronal processes (Fig. 1C). Furthermore, Dorfin colocalized not only with SOD1-positive inclusions (Fig. 1, F–I) but also with Ub in NHI in both familial (Fig. 1, J–L) and sporadic (Fig. 1, M–O) ALS. Neither neural tissues not affected in ALS nor tissues other than central nervous tissue were stained with Dorfin. Only weak staining of Dorfin was diffusely observed throughout motor neurons in normal human spinal cords without neu-

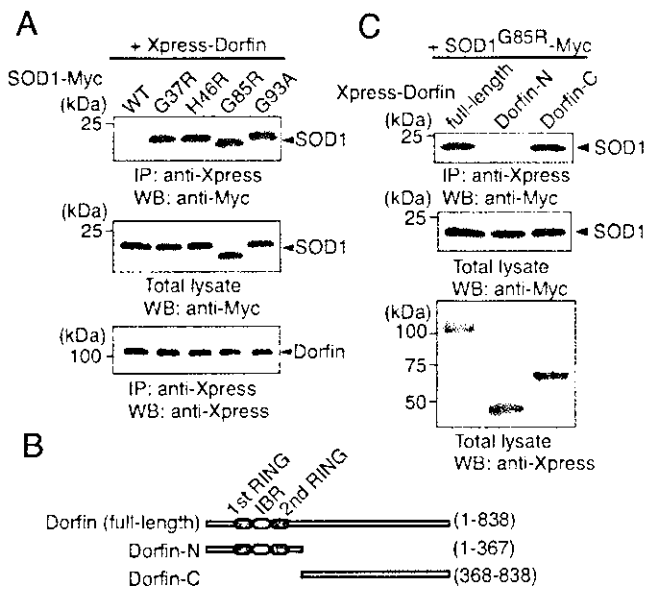


FIG. 2. Association of Dorfin with mutant SOD1 but not wild-type SOD1 in HEK293 cells. *A*, various Myc-tagged mutant SOD1s as indicated were co-transfected with Xpress-tagged Dorfin. After immunoprecipitation was performed with anti-Xpress antibody, the resulting precipitates and the cell lysate were analyzed by Western blotting with anti-Myc-HRP or anti-Xpress-HRP antibodies. Arrowheads on the right indicate the position of SOD1 or Dorfin. *B*, schematic representation of Dorfin and deletional mutants of Dorfin (*i.e.* Dorfin-N and Dorfin-C) used in this study. RING and IBR domains were schematically represented. *C*, binding of mutant SOD1 to the C-terminal portion of Dorfin. After Myc-tagged mutant-SOD1^{G85R} and Xpress-tagged full-length Dorfin or Dorfin-mutants were transfected, immunoprecipitation and Western blotting were performed as described in *A*.

rologic disease and non-transgenic littermate mice (data not shown). These findings suggest that Dorfin is involved in inclusion body formation via the ubiquitylation of substrate(s) yet to be identified in NHI and that SOD1 is a plausible target for ubiquitylation by Dorfin in familial ALS.

Dorfin Interacts with Mutant SOD1 but Not Wild-type SOD1—We examined whether Dorfin interacts with SOD1 *in vivo*. To this end, Xpress-tagged Dorfin was coexpressed with C-terminal Myc-tagged wild-type or various mutant forms of SOD1 in HEK293 cells. Western blotting analysis revealed that Dorfin co-immunoprecipitated with all mutant SOD1s examined here but not with wild-type SOD1 (Fig. 2*A*). However, Dorfin failed to bind either of the androgen receptors with normal (Q24) and extended (Q97) polyglutamine tracts or wild-type and mutant (A30P, A53T) α -synuclein (data not shown). Dorfin has a unique primary structure containing a RING finger/IBR motif at its N terminus and can be structurally divided into two parts, *i.e.* the N-terminal region containing a RING finger/IBR motif (Dorfin-N) that interacts with E2 and the C-terminal region with no similarity to any other known proteins (Dorfin-C) (Fig. 2*B*). We found that Dorfin-C but not Dorfin-N specifically bound mutant SOD1^{G85R} (Fig. 2*C*), indicating that Dorfin binds to the mutant SOD1 via its C-terminal region.

Dorfin Ubiquitylates Mutant SOD1 *In Vitro* and Promotes Ubiquitylation and Degradation of SOD1 *In Vivo*—Physical interaction between Dorfin and mutant SOD1 prompted us to investigate whether SOD1 itself is ubiquitylated by Dorfin. We first examined whether SOD1 is ubiquitylated in a culture cell model. C-terminal Myc-tagged wild-type or mutant SOD1 was co-transfected with FLAG-tagged Ub in HEK293 cells. When SOD1 was immunoprecipitated after treatment with the proteasome inhibitor MG132, all mutant SOD1s, unlike wild-type

SOD1, were found to be polyubiquitylated (Fig. 3*A*). In addition, ectopic expression of Dorfin increased the ubiquitylation of mutant SOD1^{G85R} without affecting the wild-type SOD1 (Fig. 3*B*).

We next examined whether Dorfin directly ubiquitylates SOD1 *in vitro*. For this purpose, we prepared IP Xpress-Dorfin or its deletion mutants and IP wild-type or mutant SOD1^{G85R}-Myc without proteasome inhibitor after transfection into HEK293 cells, independently. When these immunoprecipitates were incubated with recombinant E1, E2 (UbcH7), His-tagged Ub, and ATP, high molecular weight ubiquitylated bands were observed in the presence of IP-Xpress-Dorfin with mutant SOD1^{G85R}, whereas no signal was noted in wild-type SOD1 or mutant SOD1^{G85R} in the absence of either Dorfin, E1, or E2 (Fig. 3*C*). Deletion mutants of Dorfin (Dorfin-N or Dorfin-C) did not show a significant activity upon ubiquitylation against mutant SOD1^{G85R} (Fig. 3*C*), indicating that both E2-recruiting N-terminal and substrate-binding C-terminal portions are required for Dorfin-mediated ubiquitylation. Further *in vitro* studies using other mutants showed that Dorfin also ubiquitylated SOD1^{G37R} and SOD1^{G93A} significantly and ubiquitylated SOD1^{H46R} as well, although to a lesser extent (Fig. 3*D*).

Mutant SOD1 protein has a short half-life compared with wild-type SOD1 as shown previously by pulse-chase experiments (30, 32, 33). By blocking the ubiquitin-proteasome pathway, its half-life can be elongated (30, 33). We examined whether the *in vivo* stability of wild-type and mutant SOD1 is affected by Dorfin. We used pulse-chase analysis to evaluate the stability of wild-type and mutant Myc-tagged SOD1 expressed in HEK293 cells in the presence or absence of Dorfin. Pulse-chase experiments revealed that ³⁵S-labeled SOD1^{G85R} was fairly unstable compared with its wild-type version, and the degradation of SOD1^{G85R} was greatly accelerated when Dorfin was overexpressed, whereas the stability of wild-type SOD1 was unaffected (Fig. 3*E*).

Dorfin Protects Neuronal Cells from Mutant SOD1-mediated Neurotoxicity through Its E3 Activity and Reduces SOD1 Inclusion Bodies—Based on these observations, we inferred that Dorfin protects cells against mutant SOD1-mediated neurotoxicity. To study neuronal cell death induced by mutations in SOD1, we used a mouse neuroblastoma cell line (Neuro2a) transiently transfected with wild-type and a mutant (G85R and G93A). These cells are maintained as nondifferentiated dividing cells but can be induced to differentiate to be neural cells by serum deprivation (34). We transfected SOD1 with Dorfin or LacZ into Neuro2a cells and induced neural differentiation by serum deprivation after overnight post-transfection. Co-expression of Dorfin significantly reduced the percentages of PI-positive dead cells in both mutant SOD1^{G85R}- and SOD1^{G93A}-transfected cells compared with those in cells co-expressing LacZ (Fig. 4*A*). In contrast, Dorfin-N and Dorfin-C had no protective activity, indicating that the E3 activity of Dorfin is essential for the suppression of mutant SOD1-induced neuronal cell death. We also found a similar Dorfin-dependent protective effect against the loss of neuronal cell viability evoked by mutant SOD1 using the MTT assay (Fig. 4*B*). One hypothesis argues that toxicity results from the tendency of mutant SOD1 to aggregate into the cytoplasmic inclusion bodies (35) that are evident in cultured spinal motor neurons (36) and COS7 cells (37) expressing mutant SOD1 cDNA or in motor neurons from SOD1 transgenic mice (38, 39). In our experimental model, the expression of mutant SOD1^{G85R} induced perinuclear intracytoplasmic inclusion bodies in Neuro2a cells (Fig. 4*C*, left panel). The overexpression of Dorfin significantly reduced the number of aggregates in SOD1^{G85R}-transfected Neuro2a cells (Fig. 4*C*, right panel, and 4*D*).

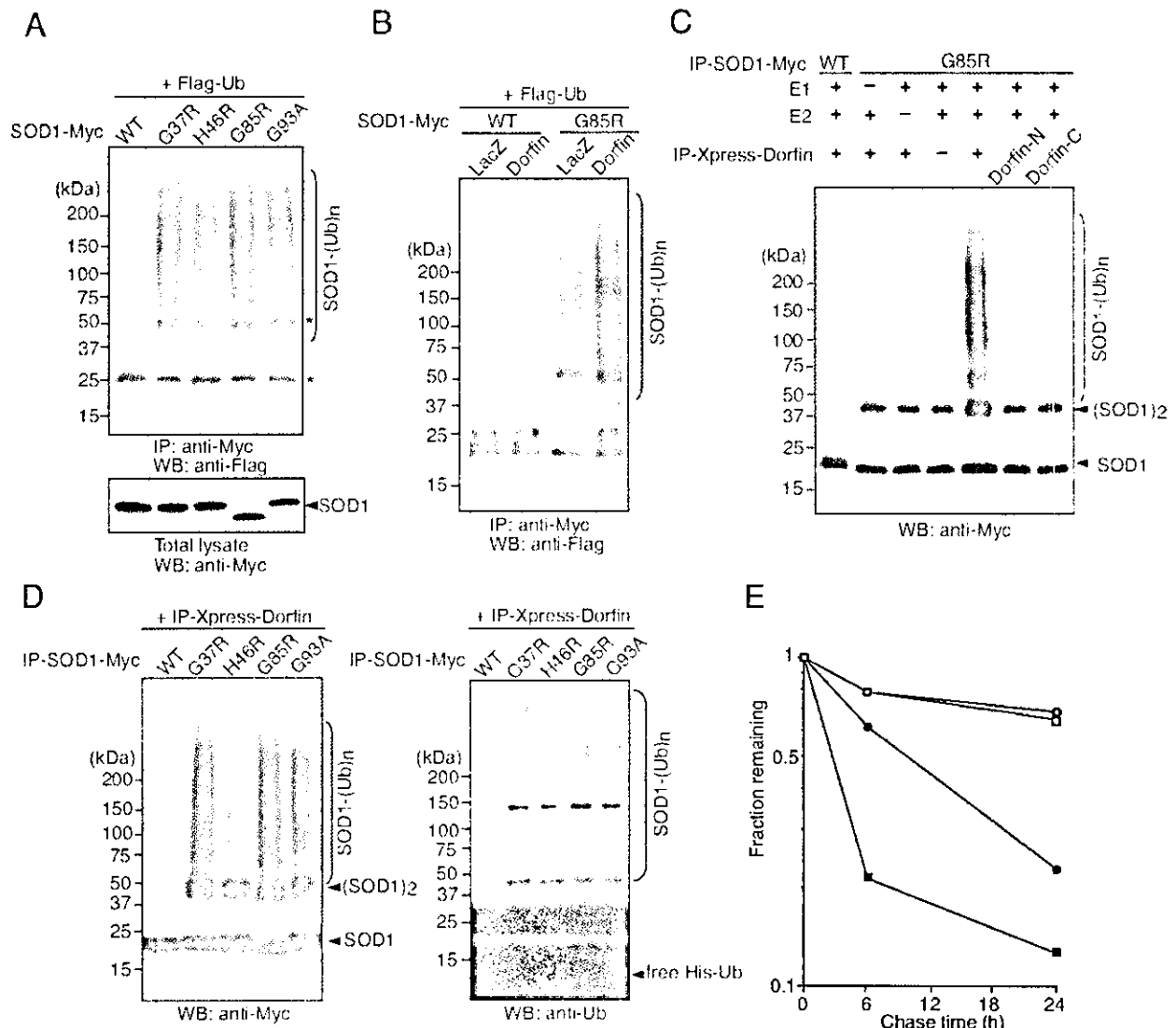


FIG. 3. Ubiquitylation of mutant SOD1 by Dorfin. *A*, mutant SOD1s were ubiquitylated in HEK293 cells, which were co-transfected with Myc-tagged wild-type SOD1 or SOD1 mutants (as indicated) and FLAG-tagged Ub. These cells were treated with $0.5 \mu\text{M}$ MG132 for 16 h after overnight post-transfection. Immunoprecipitates prepared by an anti-Myc antibody were used for immunoblotting with the anti-FLAG antibody. The high molecular-mass ubiquitylated SOD1s are shown as SOD1-(Ub)_n on the right (upper panel). Asterisks indicate IgG light and heavy chains. The blot shown is a representative blot from three independent experiments. Total lysate was used for Western blot with the anti-Myc antibody (lower panel). Asterisk on the right indicates the position of SOD1. *B*, increased ubiquitylation of SOD1^{G85R} by overexpression of Dorfin. HEK293 cells were co-transfected with Myc-tagged wild-type SOD1 or SOD1^{G85R} mutants and FLAG-tagged Ub in the presence of Dorfin or LacZ. Immunoprecipitation and immunoblotting were performed as described in *A*. *C*, *in vitro* ubiquitylation assay of SOD1^{G85R} by Dorfin. Xpress-tagged Dorfin and Myc-tagged SOD1 were transfected into HEK293 cells independently. Immunoprecipitated Dorfin (IP Xpress-Dorfin) and SOD1 (IP-SOD1-Myc) were prepared and mixed in an assay mixture for ubiquitylation. For this assay, wild-type and mutant SOD1^{G85R} and full-length Dorfin, Dorfin-N, and Dorfin-C were used. After a 90-min incubation at 30°C , SDS-PAGE was performed followed by Western blotting for SOD1 with the anti-Myc antibody. Monomeric, dimeric, and the high molecular mass-ubiquitylated SOD1 are shown on the right. Note that only mutant SOD1 showed SDS-resistant dimeric banding indicated by (SOD1)₂. *D*, *in vitro* ubiquitylation assay of various SOD1 mutants by Dorfin. The ubiquitylation assay was carried out as described in *C* except that various SOD1 mutants were used as indicated, and Western blotting was also conducted with an anti-Myc antibody (left panel) for the detection of SOD1 as well as anti-Ub antibody (right panel). *E*, accelerated degradation of mutant SOD1^{G85R} by Dorfin. HEK293 cells transiently expressing wild-type (open circles and open squares) or mutant SOD1^{G85R} (closed circles and closed squares) were pulse-labeled with [³⁵S]Cys for 45 min and chased for the time intervals indicated under the overexpression of Dorfin (open squares and closed squares) or LacZ (open circles and closed squares). Data are mean values of three independent experiments.

DISCUSSION

In the present study, we showed for the first time that mutant SOD1s are selectively degraded through a Dorfin-mediated Ub-proteasome pathway and that Dorfin protects neuronal cells against the toxic effects of mutant SOD1. Whereas Dorfin can ubiquitylate mutant SOD1s, probably because of their fragile or misfolded conformation, the constant production of high amounts of impaired SOD1 in familial ALS becomes a burden on the protein degradation process through the Ub-proteasome pathway, eventually overwhelming the capac-

ity of the proteasome to degrade toxic SOD1 and subsequently leading to the accumulation of ubiquitylated SOD1 and motor neuron death. Consistent with this scenario, recent studies reported that impairment of the Ub-proteasome system is caused by protein aggregation (40). Thus, up-regulation or exogenous expression of Dorfin may be therapeutically beneficial in familial ALS. Our results also showed that Dorfin colocalized with ubiquitylated inclusions not only in familial ALS but also in sporadic ALS. Based on this finding, it is conceivable that familial and sporadic forms of ALS share a common mechanism

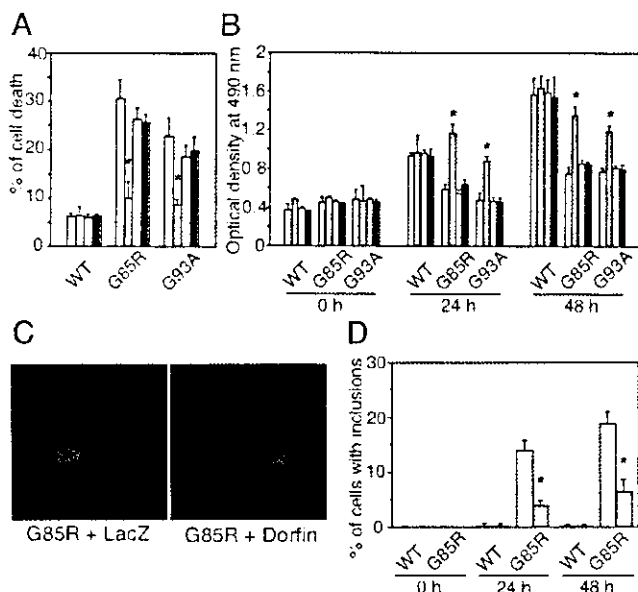


FIG. 4. Dorfin protects neural cells against mutant SOD1-mediated toxicity. *A*, cell death assay using PI staining. Neuro2a cells were grown on collagen-coated 2-chamber well slides and transfected with Myc-tagged SOD1 (wild-type, SOD1^{G85R}, and SOD1^{G93A}) and Xpress-tagged Dorfin (full-length, red bars; Dorfin-N, yellow bars; Dorfin-C, green bars). Xpress-tagged LacZ (white bars) was used as control. The pEGFP-C3 vector was also transfected as a marker of transfected cells. After 48 h of serum withdrawal, the proportions of PI- and GFP-positive cells among the GFP-positive cells were counted. Data are mean \pm S.D. values of triplicate assays. Statistical analyses were carried out by one-way analysis of variance (ANOVA). *, $p < 0.001$. *B*, the rescue effect of Dorfin expression in mutant SOD1-transfected cells on an MTT assay. Neuro2a cells were grown on collagen-coated 96-well plates and transfected as described in *A*. After changing the medium to serum-free, MTT assays were performed after 0, 24, and 48 h of incubation. Viability was measured as the level of absorbance at 490 nm. Data are mean \pm S.D. values of triplicate assays. Statistical analyses were carried out by one-way ANOVA. *, $p < 0.001$. *C* and *D*, the reduction of mutant SOD1 aggregates by Dorfin. Neuro2a cells grown on collagen-coated 2-chamber well slides were transfected with a GFP-tagged wild type or mutant SOD1^{G85R} in the presence of Dorfin (red bars) or LacZ (white bars). After 48 h of serum withdrawal, slides were examined using a laser-scanning confocal microscope. Panel *C* shows a typical example in which the overexpression of Dorfin reduces SOD1^{G85R} aggregate-bearing Neuro2a cells. The percentages of aggregate-positive cells among the GFP-positive cells were determined in *D*. Data are the mean \pm S.D. values of triplicate assays. Statistical analyses were carried out by Mann-Whitney's *U* test. *, $p < 0.01$.

involving the dysfunction of the Ub-proteasome pathway despite distinct etiological mechanisms.

Studies of parkin have provided new insights into the importance of the ubiquitin-proteasome pathway in the neuronal degeneration of PD. Parkin was shown to have E3 activity (19–21). Recently, an *O*-glycosylated form of α -synuclein and synphilin-1 were shown to be substrates of parkin (41, 42). Both α -synuclein and synphilin-1 are major components of Lewy bodies, which are ubiquitylated inclusion bodies characteristic of sporadic PD. A link between sporadic and familial PD through α -synuclein, synphilin-1, and parkin suggests that common molecular pathogenic mechanisms underlie PD. The accumulation of toxic or undesired proteins in neurons may result from the failure of degradation systems and could subsequently lead to neurodegeneration. From this point of view, in sporadic ALS post-translationally modified SOD1 (43) or other unknown substrates might accumulate in the ubiquitylated form and play a role in the pathogenesis of the disease.

Our results raise an important question related to the function of Dorfin; what is the biological role of Dorfin and how does Dorfin recognize the abnormal mutant SOD1? Because we used

IP-Dorfin and IP-mutant SOD1 for an ubiquitylating assay here, it is possible that Dorfin interacts with mutant SOD1 indirectly. Recently CHIP (carboxyl terminus of Hsc70-interacting protein), an U-box type E3, has been shown to interact with Hsp90 or Hsp70 and ubiquitylate unfolded proteins captured by these molecular chaperones in a selective manner, thus acting as a "quality control E3" (44, 45). Likewise, because Dorfin can discriminate between the normal and abnormal status of SOD1 proteins, it can be regarded as another quality control E3. However, preliminary results showed that CHIP did not ubiquitylate mutant SOD1s (data not shown); therefore, Dorfin possesses a distinct way for recognition of the abnormality of SOD1. It is possible that a novel sequence within the C terminus of Dorfin may associate with a substrate-recognizing molecule(s) (corresponding to Hsp in CHIP) or facilitate a unique mechanism for trapping the target in a direct or indirect manner. Further studies should be designed to determine this mechanism, which should enhance our understanding of Dorfin function *in vivo* and its relationship to ALS pathogenesis.

Acknowledgment—We thank Dr. J. Q. Trojanowski for helpful comments.

REFERENCES

- Tyler, H. R., and Shefner, J. (1991) in *Handbook of Clinical Neurology* (Vinken P. J., Bruyn, G. W., and Klawans, H. L., eds) Vol. 59, pp. 169–215, Elsevier Science Publishers B. V., Amsterdam
- Emery, A., and Holloway, S. (1982) in *Human Motor Neuron Diseases* (Rowland, L., ed), pp. 139–147, Raven Press, Ltd., New York
- Rosen, D. R., Siddique, T., Patterson, D., Figlewicz, D. A., Sapp, P., Hentati, A., Donaldson, D., Goto, J., O'Regan, J. P., Deng, H. X., Rahmani, Z., Krizus, A., McKenna-Yasek, D., Cayabyab, A., Gaston, S. M., Berger, R., Tanzi, R. E., Halperin, J. J., Herzfeldt, B., Van den Bergh, R., Hung, W.-Y., Bird, T., Deng, G., Mulder, D. W., Smyth, C., Laing, N. G., Soriano, E., Pericak-Vance, M. A., Haines, J., Rouleau, G. A., Gusella, J. S., Horvitz, H. R., and Brown, R. H., Jr. (1993) *Nature* **362**, 59–62
- Julien, J. P. (2001) *Cell* **104**, 581–591
- Cleveland, D. W., and Rothstein, J. D. (2001) *Nat. Rev. Neurosci.* **2**, 806–819
- Newbery, H. J., and Abbott, C. M. (2002) *Trends Mol. Med.* **8**, 88–92
- Hirano, A. (1996) *Neurology* **47**, S63–S66
- Murayama, S., Mori, H., Ihara, Y., Bouldin, T. W., Suzuki, K., and Tomonaga, M. (1990) *Ann. Neurol.* **27**, 137–148
- Leigh, P. N., Whitwell, H., Garofalo, O., Buller, J., Swash, M., Martin, J. E., Gallo, J. M., Weller, R. O., and Anderton, B. H. (1991) *Brain* **114**, 775–788
- Schiffer, D., Autilio-Gambetti, L., Chio, A., Gambetti, P., Giordana, M. T., Gullotta, F., Migheli, A., and Vighiani, M. C. (1991) *J. Neuropathol. Exp. Neurol.* **50**, 463–473
- Lowe, J. (1994) *J. Neurol. Sci.* **124**, S38–S51
- Kato, S., Takikawa, M., Nakashima, K., Hirano, A., Cleveland, D. W., Kusaka, H., Shibata, N., Kato, M., Nakano, I., and Ohama, E. (2000) *Amyotroph. Lateral Scler. Other Motor Neuron Disord.* **1**, 163–184
- Shibata, N., Hirano, A., Kobayashi, M., Siddique, T., Deng, H. X., Hung, W. Y., Kato, T., and Asayama, K. (1996) *J. Neuropathol. Exp. Neurol.* **55**, 481–490
- Niwa, J., Ishigaki, S., Doyu, M., Suzuki, T., Tanaka, K., and Sobue, G. (2001) *Biochem. Biophys. Res. Commun.* **281**, 706–713
- Morett, E., and Bork, P. (1999) *Trends Biochem. Sci.* **24**, 229–231
- Moynihan, T. P., Ardley, H. C., Nuber, U., Rose, S. A., Jones, P. F., Markham, A. F., Scheffner, M., and Robinson, P. A. (1999) *J. Biol. Chem.* **274**, 30963–30968
- Ardley, H. C., Tan, N. G., Rose, S. A., Markham, A. F., and Robinson, P. A. (2001) *J. Biol. Chem.* **276**, 19640–19647
- Kitada, T., Asakawa, S., Hattori, N., Matsumine, H., Yamamura, Y., Minoshima, S., Yokochi, M., Mizuno, Y., and Shimizu, N. (1998) *Nature* **392**, 605–608
- Shimura, H., Hattori, N., Kubo, S., Mizuno, Y., Asakawa, S., Minoshima, S., Shimizu, N., Iwai, K., Chiba, T., Tanaka, K., and Suzuki, T. (2000) *Nat. Genet.* **25**, 302–305
- Imai, Y., Soda, M., and Takahashi, R. (2000) *J. Biol. Chem.* **275**, 35661–35664
- Zhang, Y., Gao, J., Chung, K. K., Huang, H., Dawson, V. L., and Dawson, T. M. (2000) *Proc. Natl. Acad. Sci. U. S. A.* **97**, 13354–13359
- Joazeiro, C. A., Wing, S. S., Huang, H., Levenson, J. D., Hunter, T., and Liu, Y. C. (1999) *Science* **286**, 309–312
- Lorick, K. L., Jensen, J. P., Fang, S., Ong, A. M., Hatakeyama, S., and Weissman, A. M. (1999) *Proc. Natl. Acad. Sci. U. S. A.* **96**, 11364–11369
- Yang, Y., Fang, S., Jensen, J. P., Weissman, A. M., and Ashwell, J. D. (2000) *Science* **288**, 874–877
- Freemont, P. S. (2000) *Curr. Biol.* **10**, R84–R87
- Deshaies, R. J. (1999) *Annu. Rev. Cell Dev. Biol.* **15**, 435–467
- Joazeiro, C. A., and Weissman, A. M. (2000) *Cell* **102**, 549–552
- Jackson, P. K., Eldridge, A. G., Freed, E., Furstenthal, L., Hsu, J. Y., Kaiser, B. K., and Reimann, J. D. R. (2000) *Trends Cell Biol.* **10**, 429–439
- Johnston, J. A., Ward, C. L., and Kopito, R. R. (1998) *J. Cell Biol.* **143**, 1883–1898
- Johnston, J. A., Dalton, M. J., Gurney, M. E., and Kopito, R. R. (2000) *Proc.*

- Natl. Acad. Sci. U. S. A.* **97**, 12571-12576
31. Hishikawa, N., Hashizume, Y., Yoshida, M., and Sobue G. (2001) *Neuropathol. Appl. Neurobiol.* **27**, 362-372
 32. Borchelt, D. R., Lee, M. K., Slunt, H. S., Guarnieri, M., Xu, Z. S., Wong, P. C., Brown, R. H., Jr., Price, D. L., Sisodia, S. S., and Cleveland, D. W. (1994) *Proc. Natl. Acad. Sci. U. S. A.* **91**, 8292-8296
 33. Hoffman, E. K., Wilcox, H. M., Scott, R. W., and Siman, R. (1996) *J. Neurol. Sci.* **139**, 15-20
 34. Pasinelli, P., Borchelt, D. R., Houseweart, M. K., Cleveland, D. W., and Brown, R. H., Jr. (1998) *Proc. Natl. Acad. Sci. U. S. A.* **95**, 15763-15768
 35. Bruijn, L. L., Houseweart, M. K., Kato, S., Anderson, K. L., Anderson, S. D., Ohama, E., Reaume, A. G., Scott, R. W., and Cleveland, D. W. (1998) *Science* **281**, 1851-1854
 36. Durham, H. D., Roy, J., Dong, L., and Figlewicz D. A. (1997) *J. Neuropathol. Exp. Neurol.* **56**, 523-530
 37. Koide, T., Igarashi, S., Kikugawa, K., Nakano, R., Inuzuka, T., Yamada, M., Takahashi, H., and Tsuji, S. (1998) *Neurosci. Lett.* **257**, 29-32
 38. Tu, P. H., Raju, P., Robinson, K. A., Gurney, M. E., Trojanowski, J. Q., and Lee, V. M. (1996) *Proc. Natl. Acad. Sci. U. S. A.* **93**, 3155-3160
 39. Bruijn, L. I., Becher, M. W., Lee, M. K., Anderson, K. L., Jenkins, N. A., Copeland, N. G., Sisodia, S. S., Rothstein, J. D., Borchelt, D. R., Price, D. L., and Cleveland, D. W. (1997) *Neuron* **18**, 327-338
 40. Bence, N. F., Sampat, R. M., and Kopito, R. R. (2001) *Science* **292**, 1552-1555
 41. Shimura, H., Schlossmacher, M. G., Hattori, N., Frosch, M. P., Trockenbacher, A., Schneider, R., Mizuno, Y., Kosik, K. S., and Selkoe, D. J. (2001) *Science* **293**, 263-269
 42. Chung, K. K., Zhang, Y., Lim, K. L., Tanaka, Y., Huang, H., Gao, J., Ross, C. A., Dawson, V. L., and Dawson, T. M. (2001) *Nat. Med.* **7**, 1144-1150
 43. Bredesen, D. E., Ellerby, L. M., Hart, P. J., Wiedau-Pazos, M., and Valentine, J. S. (1997) *Ann. Neurol.* **42**, 135-137
 44. McClellan, A. J., and Frydman, J. (2001) *Nat. Cell. Biol.* **3**, E51-E53
 45. Murata, S., Minami, Y., Minami, M., Chiba, T., and Tanaka, K. (2001) *EMBO Rep.* **2**, 1133-1138



Adenovirus-mediated gene transfer of glial cell line-derived neurotrophic factor prevents motor neuron loss of transgenic model mice for amyotrophic lateral sclerosis

Y. Manabe, I. Nagano, M. S. A. Gazi, T. Murakami, M. Shiote, M. Shoji, H. Kitagawa, Y. Setoguchi and K. Abe

Department of Neurology, Graduate School of Medicine and Dentistry, Okayama University, Okayama, Japan (Y. Manabe, I. Nagano, M. S. A. Gazi, T. Murakami, M. Shiote, M. Shoji, K. Abe); Tokushima New Drug Research Institute, Otsuka Pharmaceutical Co. Ltd., Tokushima, Japan (H. Kitagawa); Department of Respiratory Medicine, Juntendo University School of Medicine, Tokyo, Japan (Y. Setoguchi)

Effects of adenovirus-mediated gene transfer of glial cell line-derived neurotrophic factor (GDNF) were studied in transgenic (Tg) mice model for amyotrophic lateral sclerosis (ALS). Adenoviral vector containing GDNF gene (Ad-GDNF), *E. coli lacZ* (Ad-LacZ), or vehicle was injected once a week from 35 weeks of age into the right gastrocnemius muscle of Tg mice carrying mutant human Cu/Zn superoxide dismutase (SOD1) gene, and histological analysis was performed at 46 W. Clinical data showed a tendency of improvement, but was not significantly different among the three animal groups. In contrast, total number of and phospho-Akt (p-Akt) positive large motor neurons in the treated side was significantly preserved in Ad-GDNF-treated group than in vehicle- and Ad-LacZ-treated groups ($p < 0.05$). Immunoreactivity of phospho-ERK (p-ERK) and active caspases-3 and -9 showed no difference. These results indicate that the Ad-GDNF treatment prevented motor neuron loss with preserving survival p-Akt signal and without affecting caspase activations, suggesting a future possibility for the therapy of the disease.

Keywords: adenovirus; amyotrophic lateral sclerosis; GDNF; gene therapy.

Introduction

Amyotrophic lateral sclerosis (ALS) is a neurodegenerative disease characterized by selective loss of motor neurons, causing muscular atrophy, complete paralysis and

death. A variety of mutations in Cu/Zn superoxide dismutase (SOD1) gene are present in about 20% of cases with familial ALS (FALS).¹ The toxicity of mutant SOD has been proposed to involve one or more of the following; an increase in peroxynitrite formation,^{2–4} an increase in peroxidase activity,^{5–7} and aggregation of the enzyme.⁸ A slowly degenerative death of selective neuronal population has been reported to occur under a disequilibrium between death and survival signals such as caspase-3 and Akt respectively.⁹ Although several lines of transgenic (Tg) mice have been established that express a mutant SOD1 gene and provide valuable models for human ALS,¹⁰ the primary pathogenic mechanisms of ALS remain to be elucidated.

In vivo and *in vitro* experiments have suggested that motor neuron diseases might benefit from neurotrophic factor administration.¹¹ For example, brain-derived neurotrophic factor (BDNF), neurotrophin-3 (NT-3), ciliary neurotrophic factor (CNTF), and glial cell line-derived neurotrophic factor (GDNF) protected motor neurons from acute death induced by peripheral nerve axotomy in neonate rodents.^{12,13} GDNF is the most potent protector for motor neuron, and is present at a high level in embryonic limb and muscle at the time of innervation.¹⁴ GDNF prevents motor neuron degeneration in mouse line with progressive motoneuropathy in the *pnn* mouse.¹⁵ However, the effects of GDNF on motor neuron degeneration in a genetic mouse model of FALS have not been reported.

Since the neuropathology of motor neurons in these mice develops over several months, consistent delivery of GDNF may be necessary to show an evident effectiveness. Adenoviral vectors represent an interesting means to achieve high and stable expression of neurotrophic factors *in vivo*.^{16,17} In this study, we treated Tg mice carrying an

Correspondence to: Yasuhiro Manabe, Department of Neurology, Graduate School of Medicine and Dentistry, Okayama University, 2-5-1 Shikata-cho, Okayama 700-8558, Japan. Tel: (81)-86-235-7365; Fax: (81)-86-235-7368; e-mail: manabe@cc.okayama-u.ac.jp

ALS-linked mutant SOD1 gene with intramuscular adenoviral gene transfer of GDNF, and observed a histological improvement.

Materials and methods

The recombinant adenoviral vector used in this study was based on type 5 adenovirus that was essentially the same as in previous reports.^{18,19} In brief, the E3 region of the adenovirus genome was deleted, and a cassette containing cDNA for mice GDNF or *Escherichia coli lacZ* (used as a control vector) driven by cytomegalovirus promoter and SV40 polyadenylation signal was inserted into the E1 region of the adenovirus genome by homologous recombination. With this promoter, the mice GDNF or *E. coli lacZ* gene of the episomally located adenovirus vector may be transcribed as mRNA in the nucleus, and the mRNA translated into the protein in the cytoplasm. The adenoviral vector, designated as Ad-GDNF or Ad-LacZ, was propagated in 293 cells (CRL1573; American Type Collection) and purified and titered as previously described.^{18,19}

Tg mice expressing a mutant human SOD1 with a Gly⁹³ → Ala (G93A-Tg) substitution were used in this study,^{10,20} and the G93A-Tg progeny was identified by polymerase chain reaction (PCR) amplification according to our previous reports.^{20,21} Ad-GDNF, Ad-LacZ (10⁸ plaque forming units (p.f.u.) in 10 μL of vector vehicle consisting of 10 mmol/L Tris-HCl, pH 7.4, 1 mmol/L MgCl₂, and 10% glycerol), or vehicle solution was injected into the right gastrocnemius muscle at 35 (presymptomatic, *n* = 5) weeks age mice. At around 39–40 weeks of age, the Tg mice developed progressive paralysis beginning with a posterior limb leading to death about 8 weeks later. Therefore, the GDNF gene therapy started at 35 W for applying human in the future. To evaluate clinical effects of Ad-GDNF, body weight, clinical grade (CG, normal, 1; slightly symptomatic, 2; symptomatic, 3; heavy symptomatic, 4; death, 5), rolling number of circular cage (CCR), and grasping on a rolling column (RC) were measured at 35, 40, 42, and 46 W. The CCR was measured as a voluntary movement of mice in an unilateral direction (forward or back) for 30 min in the narrow circular cage, which represents a locomotor activity of the mice. For RC, the rate of rolling of the transverse column (rota rod, diameter 3.5 cm, Acceler Rota-Rod 7650, UGO BASILE, Varese, Italy) was accelerated from 0 to 10/min.²¹ The total rolling number before they fall down was recorded as an indicator of grasping power of the mice. All experimental protocols and procedures were approved by the Animal Committee of the Okayama University Graduate School of Medicine and Dentistry, Japan.

For measurement of free-GDNF protein content, serum was collected as a sample for GDNF enzyme-linked im-

munoassay with a chicken polyclonal antibody for human GDNF was performed in the 96-well immunoassay plate (Nunc MaxiSorp Nalge Nunc Int., Rochester, NY, U.S.A), which was precoated with the anti-GDNF monoclonal antibody, using the kit (GDNF E_{max} Immunoassay System, Promega). After overnight incubation at 4°C, reaction of a second antibody-HRP conjugate (kit component) for chicken IgY was performed, followed by color development with TMB solution (kit component). After the stop reaction with 1 mol/L phosphoric acid, OD₄₅₀ was measured by a 96 well plate reader, and GDNF protein content of each sample was calculated. Using this system, immunoreactive GDNF in the sample can be quantitated in the range of 16 to 1,000 pg/mL.

For histological study, mice were decapitated with a deep anesthesia by ether at the end of experiment (48 weeks), and the lumbar spinal cord was removed and quickly frozen in a powdered dry ice. Transverse sections of 10 μm thickness were cut on a cryostat at -20°C, and were stained with hematoxylin and eosin (HE). The sections were examined by light microscope. For immunohistochemistry, the sections were treated with a rabbit polyclonal antibody specific for phospho-Akt (p-Akt, 1: 50, #9277, Cell Signaling Technology, MA), phospho-ERK (p-ERK, 1: 100, #9101, Cell Signaling Technology, MA), mouse anti-cleaved caspase-3 polyclonal antibody (1: 50, #9661, Cell Signaling Technology, MA), or rabbit anti-cleaved caspase-9 polyclonal antibody (1: 50, #9501, Cell Signaling Technology, MA) in 10% normal rabbit serum and 0.3% Triton X-100 at 4°C for 16 h, and developed by the standard avidin-biotin complex method as our previous report.²² For quantification of immunohistochemistry, the average optical densities were measured using a computer-based system (NIH Image Ver. 1.62, NIH, USA). The background density was subtracted from the positive signal. The species specificity of the secondary antibody was verified by omitting the primary antibodies.

Number of large ventral horn neurons was measured on the spinal cord sections. At least five transverse sections from each lumbar cord were examined by light microscope. The number in anterior horn areas in each section was combined and averaged in order to provide the number of neurons in bilateral anterior horns per section. Values are expressed as mean ± SE. Comparisons of vehicle and drug-treated groups were made with a non-parametrical test such as the Wilcoxon rank-sum (Wilcoxon's U) test for a part of clinical data (CG, body weight, CCR, and RC) and biological data.

Results

At around 39–40 weeks of age, the Tg mice developed progressive paralysis beginning with a posterior limb.

Figure 1. Clinical data in CG, CCR, and RC indicate no significant difference between vehicle-, Ad-LacZ-, and Ad-GDNF-treated groups. Data represent mean \pm SE.

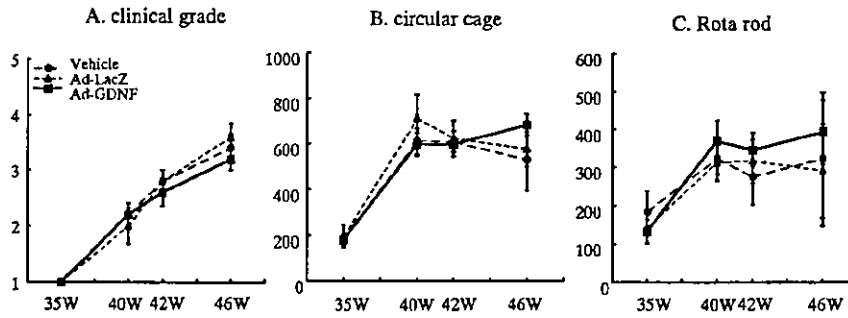
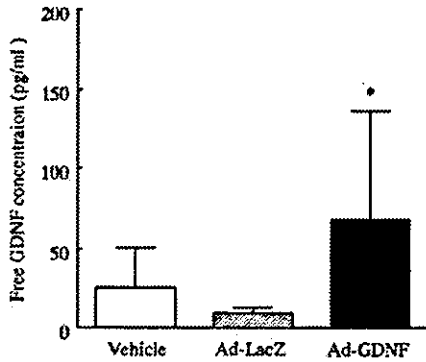


Figure 2. Serum level of GDNF by ELISA assay after treatment. Serum level of GDNF was significantly higher in Ad-GDNF-treated group than that in the vehicle- and Ad-LacZ- treated groups ($n = 5$, $*p < 0.05$). Data represent mean \pm SE.



Although clinical data in CG, CCR, and RC showed no significant difference between vehicle-, Ad-LacZ-, and Ad-GDNF-treated groups, there were tendency of improvements in three clinical scores in Ad-GDNF group

(Figure 1, solid lines) compared to other two groups (Figure 1). With ELISA assay, serum level of GDNF was higher in Ad-GDNF-treated group than the vehicle- and Ad-LacZ-treated groups ($n = 5$, $*p < 0.05$, Figure 2).

In the HE staining (Figures 3A and 4), number of the large motor neuron in the treated side was significantly preserved in Ad-GDNF-treated group (Figures 3A and 4e) than in vehicle- (Figure 4a) and Ad-LacZ- (Figure 4c) treated groups ($*p < 0.05$). Immunoreactivity of p-Akt was present predominantly in the neuronal cytoplasm (Figure 5A, arrows), and the number of p-Akt positive large motor neurons was significantly higher in the treated side of Ad-GDNF-treated group than in vehicle- and Ad-LacZ-treated groups (Figure 3B, $*p < 0.05$; 5A, arrows). Immunoreactivity of p-ERK was present predominantly in the nucleus and/or perinucleus (Figure 5B, arrows), but number of p-ERK positive large motor neurons was not different in the three groups (Figure 5B).

In contrast, immunoreactivity of active caspases-3 and -9 showed no significant difference between vehicle-, Ad-LacZ-, and Ad-GDNF-treated groups (Figures 6A and

Figure 3. (A) HE stainings show a preserved number of the ipsilateral large motor neurons (R) in Ad-GDNF- than in vehicle- and Ad-LacZ-treated groups ($*p < 0.05$). Data represent mean \pm SD. WT, wild type. R: right side, L: left side. (B) P-Akt stainings show a preserved number of the ipsilateral large motor neurons (R) in Ad-GDNF- than in vehicle- and Ad-LacZ-treated groups ($*p < 0.05$). Data represent mean \pm SD. R: right side, L: left side.

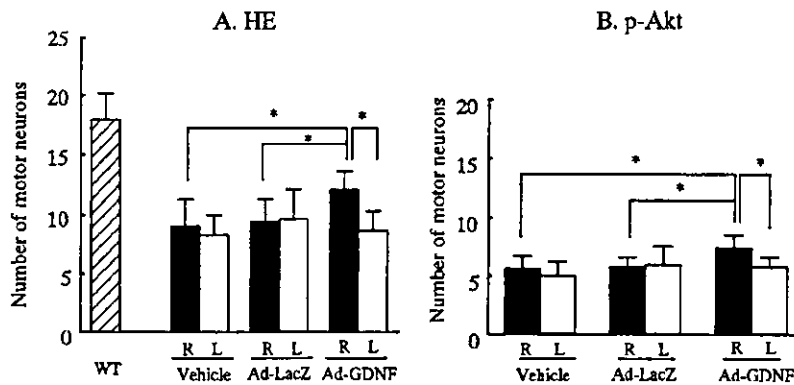
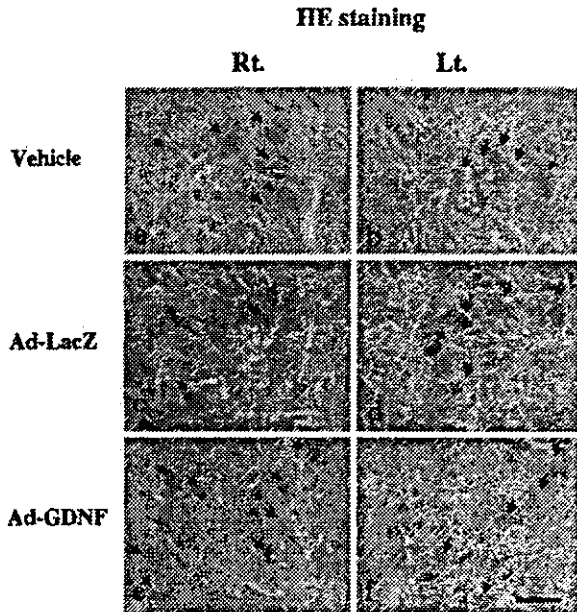
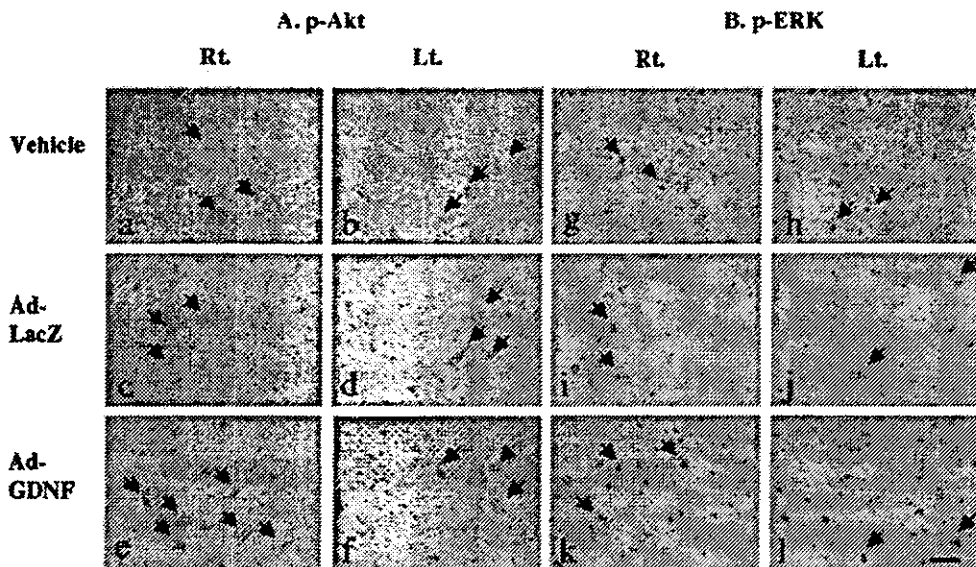


Figure 4. Representative microphotographs of HE staining show a significant preservation of large motor neurons in the treated side (Rt) of Ad-GDNF-treated group than in vehicle- and Ad-LacZ-treated groups (a,c,e, arrows * $p < 0.05$). Scale bars: 100 μ m.



B, arrows). Any cells in the posterior horn did not show obvious immunoreactivity for the antibodies (not shown), and the sections without the primary or secondary antibody gave no staining (not shown).

Figure 5. Immunohistochemistry for p-Akt (A) shows a predominant location of p-Akt in the cytoplasm (A, arrows), and preserved number of p-Akt positive large motor neurons in the treated side in Ad-GDNF-treated group (A, a,c,e, arrows). Immunohistochemistry for p-ERK (B) shows a predominant location of p-ERK in the nucleus and/or perinucleus (B, arrows), but no significant difference in the number of positive large motor neurons in three groups. Scale bars: 100 μ m.

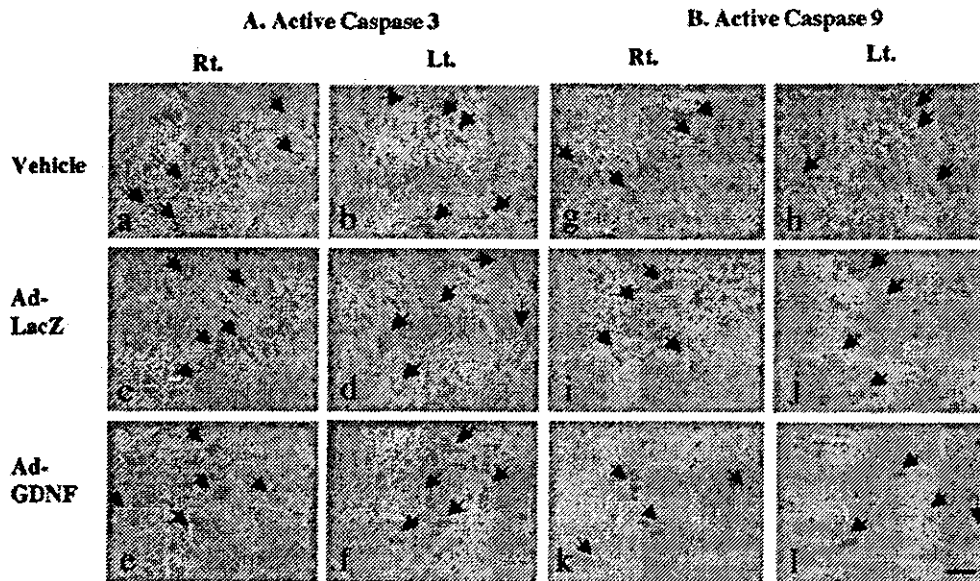


Discussion

In the present study, number of motor neuron and immunoreactivity of p-Akt were significantly preserved in Ad-GDNF-treated group than in vehicle- and Ad-LacZ-treated groups (Figures 3–5). The intramuscular injection of Ad-GDNF to Tg mice resulted in the long-term expression of adenoviral GDNF with elevated serum level (Figure 2). The Ad-GDNF treatment prevented motor neuron loss with preserving p-Akt staining (Figure 5A) and without affecting p-ERK and caspases-3 and -9 (Figures 5B and 6). Because contralateral side (Lt) did not show such a protective effect (Figures 3–5), the effect of Ad-GDNF was not simply due to serum elevation of GDNF (Figure 2), but possibly to a retrograde transport of adenovirus that expressed GDNF in the motor neurons. The present results are consistent with such previous findings as early and progressive loss of survival signals phosphatidylinositol-3 kinase (PI3K) and Akt, and as late activation of caspase-3 in this Tg mice.⁹

Recent studies showed that BDNF, NT-3, CNTF, and cardiotrophin-1 supported survival of embryonic motor neurons in culture.^{11,15,23} CNTF, NT-3, and BDNF, as well as GDNF, prevented motor neuron death in mouse models of motor neuron disease, such as wobbler and *pnu* mice.¹⁵ GDNF was protective against motor neuron injury after axotomy of peripheral nerves in neonatal rats with adenoviral gene transfer. Grafting of GDNF-secreting myoblasts into two hindlimb muscles of a mouse model for ALS protected the innervating motor neurons from degeneration and delayed the onset of the disease

Figure 6. Immunohistochemistry for active caspase-3 (A) and -9 (B) show no significant difference between vehicle-, Ad-LacZ-, and Ad-GDNF-treated groups (A,B, arrows). Scale bars: 100 μ m.



symptoms.²⁴ This is the first report of a therapeutic effect of the intramuscular injection of Ad-GDNF in Tg model mice for ALS.

Both PI3K and its key downstream molecule Akt play a critical role in neuronal survival, and are supported by neurotrophic factors such as nerve growth factor (NGF) and insulin-like growth factor-1 (IGF-1).²⁵ Akt prevents apoptosis of many cells under pathological conditions.^{26,27} The signaling through PI3K/Akt may be the most important pathway for neuronal survival. Our study indicates that the Ad-GDNF treatment prevented motor neuron loss through preserving survival signaling pathway Akt, but not affecting p-ERK and active caspases-3 and -9 immunostainings. Although clinical data in CG, CCR, and RC showed a tendency of improvement, the difference was not significant among vehicle-, Ad-LacZ-, and Ad-GDNF-treated groups (Figure 1). Because 35 W of age, when the GDNF gene therapy started, is just before the disease development, clinical improvement should become significant when the therapy started from earlier stage. Alternatively, the present results indicate that supporting survival Akt signal of motor neurons by GDNF might not be sufficient to successfully treat motor neuron disease. In fact, the maintenance of motor neurons also depends on many other different neurotrophic factors.²⁸

Because the present GDNF gene therapy started just before or at around the disease beginning for aiming to apply human ALS patients, clinical effectiveness was not strong and significant. However, GDNF gene therapy significantly prevented motor neuron loss in Tg mice model for ALS, still suggesting a possibility of GDNF

gene therapy to ameliorate the progression of human ALS. Treatment with suitable combinations of neurotrophic factors might be much more beneficial than treatment with one factor alone.

Acknowledgment

This work was partly supported by Grant-in-Aid for Scientific Research (B) 12470141, (C) 13670649 and (Hoga) 12877211 from the Ministry of Education, Science, Culture and Sports of Japan, Kobayashi Magobe Memorial Medical Foundation, and by grants (Tashiro K, Itoyama Y, and Tsuji S), and Comprehensive Research on Aging and Health (H11-Choju-010, No. 207, Koizumi A) from the Ministry of Health and Welfare of Japan.

References

- Deng HX, Hentati A, Tainer JA, *et al.* Amyotrophic lateral sclerosis and structural defects in Cu,Zn superoxide dismutase. *Science* 1993; 261: 1047-1105.
- Abe K, Pan L-H, Watanabe M, Kato T, Itoyama Y. Induction of nitrotyrosine-like immunoreactivity in the lower motor neuron of amyotrophic lateral sclerosis. *Neurosci Lett* 1995; 199: 152-154.
- Manabe Y, Wang JM, Warita H, *et al.* Glutamate enhances DNA fragmentation in cultured spinal motor neurons of rat. *Neural Res* 2001; 23: 79-82.
- Manabe Y, Wang JM, Murakami T, *et al.* Expressions of nitrotyrosine and TUNEL immunoreactivities in cultured rat spinal cord neurons after exposure to glutamate, nitric oxide, or peroxynitrite. *J Neurosci Res* 2001; 65: 371-377.

5. Ferrante RL, Browne SE, Shinobu LA, et al. Evidence of increased oxidative damage in both sporadic and familial amyotrophic lateral sclerosis. *J Neurochem* 1997; 69: 2064–2074.
6. Manabe Y, Wang JM, Warita H, Shiro Y, Abe K. Expressions of caspase-3, TUNEL, and HSP72 immunoreactivities in cultured spinal cord neurons of rat after exposure to glutamate, nitric oxide, or peroxynitrite. *Neurotox Res* 2001; 3: 281–289.
7. Manabe Y, Warita H, Murakami T, et al. Early decrease of redox factor-1 in spinal motor neurons of presymptomatic transgenic mice with a mutant SOD1 gene. *Brain Res* 2001; 915: 104–107.
8. Durham HD, Roy J, Dong L, Figlewicz DA. Aggregation of mutant Cu/Zn superoxide dismutase proteins in a culture model of ALS. *J Neuropathol Exp Neurol* 1997; 56: 523–530.
9. Warita H, Manabe Y, Murakami Y, et al. Early decrease of survival signal-related proteins in spinal motor neurons of presymptomatic transgenic mice with a mutant SOD1 gene. *Apoptosis* 2001; 6: 345–352.
10. Gurney ME, Pu H, Chiu AY, et al. Motor neuron degeneration in mice that express a human Cu,Zn superoxide dismutase mutation. *Science* 1994; 264: 1772–1775.
11. Mitsumoto H, Ikeda K, Klinkosz B, et al. Arrest of motor neuron disease in wobbler mice cotreated with CNTF and BDNF. *Science* 1994; 265: 1107–1110.
12. Oppenheim RW, Houenou LJ, Johnson JE, et al. Developing motor neurons rescued from programmed and axotomy-induced cell death by GDNF. *Nature* 1995; 373: 344–346.
13. Munson JB, McMahon SB. Effects of GDNF on axotomized sensory and motor neurons in adult rats. *Eur J Neurosci* 1997; 9: 1126–1129.
14. Henderson CE, Phillips HS, Pollock RA, et al. GDNF: A potent survival factor for motoneurons present in peripheral nerve and muscle. *Science* 1994; 266: 1062–1064.
15. Bordet T, Schmalbruch H, Pettmann B, et al. Adenoviral cardiotrophin-1 gene transfer protects pmn mice from progressive motor neuropathy. *J Clin Invest* 1999; 104: 1077–1085.
16. Abe K, Setoguchi Y, Hayashi T, Itoyama Y. *In vivo* adenovirus-mediated gene transfer and the expression in ischemic and reperfused rat brain. *Brain Res* 1997; 763: 191–201.
17. Warita H, Abe K, Setoguchi Y, Itoyama Y. Expression of adenovirus-mediated *E. coli lacZ* gene in skeletal muscles and spinal motor neurons of transgenic mice with a mutant superoxide dismutase gene. *Neurosci Lett* 1998; 246: 153–156.
18. Setoguchi Y, Danel C, Crystal RG. Stimulation of erythropoiesis by *in vivo* gene therapy: Physiologic consequences of transfer of the human erythropoietin gene to experimental animals using an adenovirus vector. *Blood* 1994; 84: 2946–2953.
19. Kitagawa H, Sasaki C, Sakai K, et al. Adenovirus-mediated gene transfer of glial cell line-derived neurotrophic factor prevents ischemic brain injury after transient middle cerebral artery occlusion in rats. *J Cereb Blood Flow Metab* 1999; 19: 1336–1344.
20. Warita H, Itoyama Y, Abe K. Selective impairment of fast anterograde axonal transport in the peripheral nerves of asymptomatic transgenic mice with a G93A mutant SOD1 gene. *Brain Res* 1999; 819: 120–131.
21. Abe K, Morita S, Kikuchi T, Itoyama Y. Protective effect of a novel free radical scavenger, OPC-14117, on wobbler mouse motor neuron disease. *J Neurosci Res* 1997; 48: 63–70.
22. Warita H, Hayashi T, Murakami T, Manabe Y, Abe K. Oxidative damage to mitochondrial DNA in spinal motoneurons of transgenic ALS mice. *Mol Brain Res* 2001; 89: 147–152.
23. Haase G, Kunnell P, Pettman B, et al. Gene therapy of murine motor neuron disease using adenoviral vectors for neurotrophic factors. *Nat Med* 1997; 3: 429–436.
24. Mahajeri MH, Figlewicz DA, Bohn MC. Intramuscular grafts of myoblasts genetically modified to secrete glial cell line-derived neurotrophic factor prevent motoneuron loss and disease progression in a mouse model of familial amyotrophic lateral sclerosis (FALS). *Hum Gene Ther* 1999; 3: 1853–1866.
25. Dudek H, Datta SR, Franke TF, et al. Regulation of neuronal survival by the serine-threonine protein kinase Akt. *Science* 1997; 275: 661–665.
26. Datta SR, Dudek H, Tao X, et al. Akt phosphorylation of BAD couples survival signals to the cell-intrinsic death machinery. *Cell* 1997; 91: 231–241.
27. Kauffmann-Zeh A, Rodriguez-Viciana P, Ulrich E, et al. Suppression of c-Myc-induced apoptosis by Ras signalling through PI(3)K and PKB. *Nature* 1997; 385: 544–548.
28. Sagot Y, Tan SA, Hammang JP, Aebischer P, Kato AC. GDNF slows loss of motoneurons but not axonal degeneration or premature death of pmn/pmn mice. *J Neurosci* 1996; 16: 2335–2341.

VENTRAL ROOT AVULSION LEADS TO DOWNREGULATION OF GluR2 SUBUNIT IN SPINAL MOTONEURONS IN ADULT RATS

I. NAGANO,^{a,b,c*} T. MURAKAMI,^b M. SHIOTE,^b K. ABE^b AND Y. ITOYAMA^c

^aNeurology Service, National Yonezawa Hospital, 26100-1 Misawa, Yonezawa, Yamagata, Japan

^bDepartment of Neurology, Okayama University Medical School, 2-5-1 Shikata-cho, Okayama, 700-8558 Japan

^cDepartment of Neurology, Tohoku University School of Medicine, 2-1 Seiry-cho, Aoba-ku, Sendai, Miyagi, 980-0872, Japan

Abstract—It has been observed that motor neuron death is induced in adult rats by ventral root avulsion which involves pulling out the spinal cord root. Since motor neurons are reported to be selectively vulnerable to α -amino-3-hydroxy-5-methyl-4-isoxazole propionate receptor-mediated injury *in vitro*, we investigated changes in the expression of α -amino-3-hydroxy-5-methyl-4-isoxazole propionate-receptor subunits in rat spinal motor neurons after ventral root avulsion. The L4–L5 ventral roots of adult Sprague–Dawley rats were avulsed by an extravertebral extraction procedure. After an appropriate survival time, α -amino-3-hydroxy-5-methyl-4-isoxazole propionate-receptor subunits were detected immunohistochemically in the L4–L5 segments. Ventral root avulsion resulted in a 60% loss of motor neurons by 14 days after surgery. GluR2 labeling in motor neurons was markedly decreased after avulsion, but before the onset of motor neuron death, while the GluR1 and GluR4 labeling of motor neurons remained unchanged. Intrathecal administration of α -amino-3-hydroxy-5-methyl-4-isoxazole propionate-receptor antagonists rescued a significant number of injured motor neurons from cell death. In contrast, *N*-methyl-D-aspartate-receptor antagonists did not prevent motor neuron death. Since the presence of GluR2 subunit renders heteromeric α -amino-3-hydroxy-5-methyl-4-isoxazole propionate receptors Ca^{2+} -impermeable, the downregulation of GluR2 may result in increased formation of GluR2-lacking, Ca^{2+} -permeable α -amino-3-hydroxy-5-methyl-4-isoxazole propionate receptors in motor neurons and could contribute to motor neuron death after ventral root avulsion. © 2003 IBRO. Published by Elsevier Science Ltd. All rights reserved.

Key words: AMPA receptors, GluR2, glutamate receptors, motor neuron spinal cord.

*Correspondence to: I. Nagano, Department of Neurology, Okayama University Medical School, 2-5-1 Shikata-cho, Okayama, 700-8558 Japan. Tel: +81-86-235-7365; fax: +81-86-235-7368.

E-mail address: inagano@cc.okayama-u.ac.jp (I. Nagano).

Abbreviations: aCSFm, artificial cerebrospinal fluid; ALS, amyotrophic lateral sclerosis; AMPA, α -amino-3-hydroxy-5-methyl-4-isoxazole propionate; CNQX, 6-cyano-7-nitroquinoxaline-2,3-dione; DAB, 3,3'-diaminobenzidine; D-AP5, *D* (-)-2-amino-5-phosphonopentanoic acid; mRNA, messenger RNA; MK-801, 5-methyl-10,11-dihydro-5H-dibenzo[*a,d*]cyclohepten-5,10-imine; NBQX, 1,2,3,4-tetrahydro-6-nitro-2,3-dioxo-benzof[*q*]quinoxaline-7-sulfonamide; NMDA, *N*-methyl-D-aspartate; SOD, superoxide dismutase.

0306-4522/03/30.00+0.00 © 2003 IBRO. Published by Elsevier Science Ltd. All rights reserved.
doi:10.1016/S0306-4522(02)00816-3

Transection of axons of motor neurons during early neonatal development results in massive motor neuron cell loss, whereas axotomy of adult peripheral nerve induces little, if any, neuronal death (Schmalbruch, 1984). A different type of lesion, ventral root avulsion, which involves pulling the root out of the spinal cord, induces the death of virtually all motor neurons in the adult rat (Koliatsos et al., 1994). In humans, brachial plexus root avulsion results in permanent disability of a paralyzed extremity unless continuity is restored between the spinal cord and nerve roots (Doi et al., 2002). Martin et al. have recently reported that motor neuron death following avulsion injury has some of the characteristics of apoptosis (Martin et al., 1999a), which resembles motor neuron degeneration in human amyotrophic lateral sclerosis (ALS) (Martin, 1999b). ALS is a progressive, fatal neurodegenerative disease and characterized by the selective loss of motor neurons in the spinal cord, brainstem and motor cortex. Up to 10% of ALS cases are familial, and approximately 25% of these are linked to mutation in superoxide dismutase (SOD) 1, an antioxidant enzyme that protects cells against superoxide toxicity (Rosen et al., 1993). Over the years, a variety of studies, including investigations of SOD1-mutant mice that develop motor neuron disease (Gurney et al., 1994; Wong et al., 1995), have established that mutant SOD1 causes motor neuron loss through the gain of toxic properties (Cleveland and Rothstein, 2001). However, the mechanisms underlying the selective degeneration of motor neurons in familial and sporadic ALS still remain unknown. Avulsion injury can possibly be used as a model for assessing the mechanisms of motor neuron death occurring in ALS and for testing the *in vivo* effects of various therapeutic agents on degenerating motor neurons.

Glutamate excitotoxicity has been implicated in the pathogenesis of motor-neuron death both *in vitro* and *in vivo* (Hugon et al., 1989; Rothstein and Kundl, 1995b; Carriedo et al., 1996). In ALS patients, considerable increases in the levels of glutamate have been found in the cerebrospinal fluid, indicating abnormalities in glutamate handling (Rothstein et al., 1990; Shaw et al., 1995). Direct measurement of functional glutamate transport in ALS revealed a marked diminution in the affected brain and spinal cord regions, which was the result of a pronounced loss of the astroglial glutamate transporter (Rothstein et al., 1995a). Thus, glutamate toxicity would also play a role in the pathogenesis of ALS. Although *N*-methyl-D-aspartate (NMDA) receptors may mediate the most acute neuronal injuries, α -amino-3-hydroxy-5-methyl-4-isoxazole propionate (AMPA) receptors seem to be of great importance to the slow degeneration of motor neurons (Weiss and Choi,

1991). Supporting this hypothesis, motor neurons are selectively vulnerable to AMPA receptor-mediated injury *in vitro* (Carriedo et al., 1996), and selective AMPA-receptor antagonists protect motor neurons against the degeneration caused by chronic blockade of the glutamate uptake in spinal cord culture (Rothstein et al., 1993). AMPA receptors containing the GluR2 subunit exhibit low Ca^{2+} permeability, whereas AMPA receptors lacking GluR2 are much more Ca^{2+} -permeable (Iino et al., 1990; Brorson et al., 1992; Burnashev et al., 1992). It has been reported that GluR2 messenger RNA (mRNA) is preferentially decreased in CA1 neurons after transient global ischemia but before neuronal cell death (Gorter et al., 1997). The authors anticipated that this reduction in GluR2 expression would facilitate toxic AMPA-mediated Ca^{2+} entry into CA1 neurons and be relevant to the neuronal cell death. Thus, it is conceivable that glutamate toxicity via GluR2-lacking AMPA receptors would be implicated in the motor neuron death induced by avulsion injury and possibly in ALS. To verify this hypothesis, we examined the change in the expression of AMPA receptor subunits in the spinal motor neurons of avulsed rats, and investigated whether the change was related to motor-neuron death following avulsion injury.

EXPERIMENTAL PROCEDURES

Animal surgery and motoneuron counting

All procedures were approved and in accord with guidelines set by our Institutional Animal Care and Use Committee. All possible efforts were made to minimize the number of animals used and their suffering. Male Sprague–Dawley rats (250–300 g, 8–9 weeks old) were anesthetized with ketamine (50 mg/kg) and xylazine (12 mg/kg). The right L4 and L5 spinal roots of the rats were avulsed by an extravertebral procedure. The avulsed ventral and dorsal roots were cut away from the peripheral nerve and examined to confirm the success of the avulsion.

In another series of experiments, continuous infusion of various glutamate antagonists dissolved in sterile artificial cerebrospinal fluid (aCSF; NaCl 122 mM, KCl 3.1 mM, NaHCO_3 5 mM, KH_2PO_4 0.4 mM, CaCl_2 1.3 mM, MgSO_4 1.0 mM, D-glucose 10 mM, pH 7.4) into the intrathecal lumbar spinal cord region was performed in avulsed animals using miniosmotic pumps (model #2002, Alzet, Palo Alto, CA, USA; nominal infusion rate, 0.5 $\mu\text{l/h}$) attached to polyethylene cannulae. The minipump was placed subcutaneously at a lumbar site, and a rostrally directed cannula was threaded through the muscle close to the exposed region of the spinal column. A small area of muscle and vertebral bone was cleared from the dorsal L4–L5 segments, and the tip of the cannula was placed through a small incision, under the dura, and eased down the dorsal spinal cord by a pre-measured distance, to within the region of the lumbosacral segments (L6–S1). The position of the tip of the cannula with respect to the level of the spinal segment was ascertained at the end of each experiment, and only data from animals with correct cannula placement (L6–S1) were used in the analysis. MK-801 [(+)-MK-801 hydrogen maleate; RBI, Natick, MA, USA] and D (-)-2-amino-5-phosphonopentanoic acid (D-AP5; Tocris Cookson, Ballwin, MO, USA) were used as NMDA receptor antagonists, and 1,2,3,4-tetrahydro-6-nitro-2,3-dioxo-benzof[quinoxaline-7-sulfonamide (NBQX disodium; RBI) and 6-cyano-7-nitroquinoxaline-2,3-dione (CNQX disodium; RBI) were used as AMPA receptor antagonists. These antagonists were water-soluble and dissolved easily in aCSF. The concentration of the antagonists was 2 mM and the infusion rate was 1

nmole/h. As a control, aCSF was infused into avulsed animals in the same manner.

The rats were killed at 0 h ($n=3$), 24 h ($n=8$), 3 days ($n=6$), 7 days ($n=9$), 14 days ($n=9$), 21 days ($n=8$) or 28 days ($n=4$) following the avulsion injury. At the end of the survival time, the animals were anesthetized with a lethal dose of pentobarbital, and perfused with phosphate-buffered saline (pH 7.4) followed by 4% paraformaldehyde in 0.1-M phosphate buffer. The region of the spinal cord spanning L3–L6 was fixed by immersion in the fixative noted above. Serial transverse sections were cut at 10 μm through the L4–L5 segments using a cryostat. For motor neuron counting, sections were stained with Cresyl Violet (Nissl stain) and motor neurons (neurons with a diameter larger than 30 μm in the ventral horn) with clear nucleoli were counted by blind investigators in every fifth section on both sides of the spinal cord as described previously (Oppenheim, 1986).

Immunohistochemical analysis for AMPA receptor subunits

Immunohistochemical detection of each AMPA-receptor subunit was performed using a polyclonal anti-GluR1 (1.0 $\mu\text{g/ml}$), monoclonal anti-GluR2 (2.0 $\mu\text{g/ml}$), polyclonal anti-GluR2 (0.5 $\mu\text{g/ml}$), or polyclonal anti-GluR4 (1.0 $\mu\text{g/ml}$) antibody (all obtained from Chemicon, Temecula, CA, USA). These antibodies have been extensively tested and are of a high specificity (Vissavajhala et al., 1996; Bernard et al., 1997; Petralia et al., 1997; Vandenberghe et al., 2001). In addition, an NMDA receptor subunit, NR1, was also detected in the spinal cord sections using a monoclonal anti-NR1 antibody (3.6 $\mu\text{g/ml}$; Chemicon). The immunohistochemical staining was developed using a Vector ABC kit (Vector Laboratory, Burlingame, CA, USA) with 3,3'-diaminobenzidine (DAB) as the chromogen. After DAB treatment, all sections were washed and coverslipped without counterstaining. For each AMPA-receptor subunit, every tenth section through the L4–L5 segments was immunostained and the number of motor neurons positive for each subunit was counted by blind investigators.

RESULTS

Motoneuron loss following avulsion

L4 and L5 nerve root avulsion lead to profound retrograde degeneration of the corresponding spinal motor neurons (Fig. 1). While no apparent cell loss was observed at 24 h and 3 days after avulsion, 1 week after injury there was a 36% motoneuron loss on the lesion side of the spinal cord (Fig. 2). However, morphological changes such as cell shrinkage and nuclear pyknosis were observed 3 days after avulsion. At day 14, more than 56% of the motor neurons had degenerated. The cell loss steadily continued and by 4 weeks there was a 78% loss of the motor neurons. In addition, extensive gliosis was observed on the side of the lesion.

GluR2 expression is decreased in motoneurons after avulsion

In unlesioned spinal cord, GluR2 was highly expressed in the substantia gelatinosa and superficial laminae of the dorsal horn, and was also present in the motor neurons in the ventral horn (Fig. 3). At high magnification, immunoreactivity for GluR2 was observed in the cell bodies and dendrites (Fig. 4A) of motor neurons. GluR1 immunoreactivity was strong in the superficial laminae of the dorsal horn, with low levels in the ventral motor neurons (data not

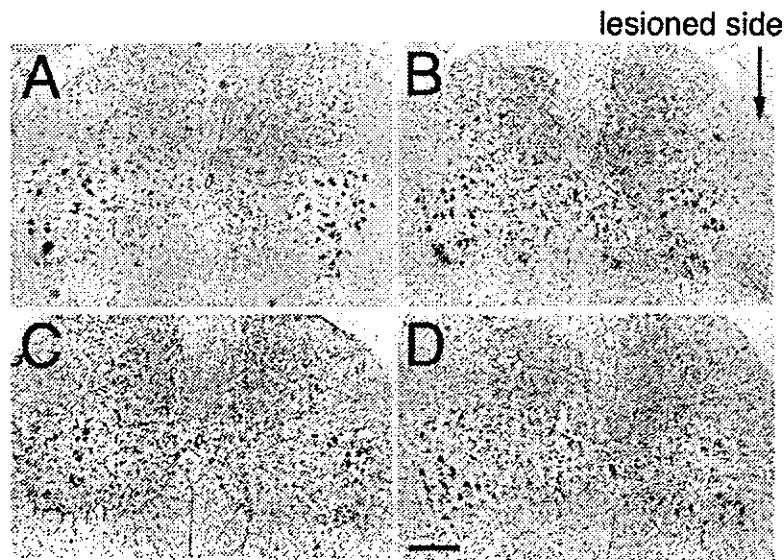


Fig. 1. Cresyl Violet (Nissl)-stained sections show the effects of ventral root avulsion in L4–L5 spinal motor neurons. Motoneuron loss on the lesioned side is apparent at 7 days after avulsion. (A) 0 h, (B) 3 days, (C) 7 days, and (D) 14 days after avulsion. Scale bar in D=400 μ m (also applies to A, B and C).

shown). GluR4 was detectable in the substantia gelatinosa, with moderate to strong labeling of the ventral motor neurons (data not shown). Immunoreactivity for NR1 was found in neurons throughout the spinal gray matter, with motor neurons being weakly positive (data not shown).

Twenty-four hours after avulsion, the number of GluR2-positive motoneurons had significantly decreased on the lesion side of the spinal cord to $82.9 \pm 7.8\%$ of the number of GluR2-positive motoneurons on the intact side,

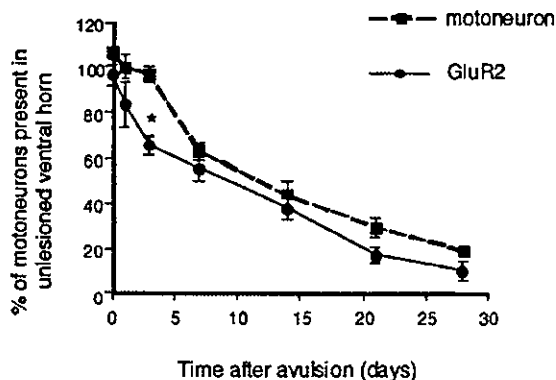


Fig. 2. No apparent cell loss is detected at 1 or 3 days after avulsion. One week after injury a 36% cell loss is observed on the lesioned side. By 4 weeks, there is a 78% loss of motoneurons. The number of GluR2-positive motoneurons is significantly decreased at 3 days after avulsion. One and 2 weeks after avulsion, GluR2 expression is markedly reduced, to 54.3 ± 4.4 and $38.5 \pm 4.9\%$ of the intact side, respectively. Thus, the reduction in GluR2 expression in motoneurons precedes motoneuron death. Data are expressed as the percentage (mean \pm S.E.M.) of the contralateral (control) motoneuron numbers, which represent 100%. * $P < 0.01$ versus number of surviving motoneurons at 3 days postlesion, and GluR2-positive motoneurons at 0 h. Statistical comparisons were performed using one-way analysis of variance followed by Newman-Keuls test.

suggesting that downregulation of GluR2 preceded motor neuron death (Figs. 2 and 3). Three and 7 days after avulsion, GluR2-positive motoneurons were markedly reduced on the lesion side to $64.1 \pm 5.2\%$ and $54.3 \pm 4.4\%$ of motoneurons on the intact side, respectively (Figs. 2, 3 and 4). In contrast, there were no conspicuous changes in GluR2 expression in other neurons including the dorsal horn neurons and interneurons in the ventral horn. No obvious changes in the staining of the motor neurons were detected for the other subunits, GluR1, GluR4 and NR1, 3 days after avulsion (Fig. 5).

Effects of glutamate receptor antagonists on lesioned motoneurons

Treatment of avulsion-lesioned rats with the AMPA receptor antagonists, NBQX and CNQX, rescued a significant number (20%) of injured motoneurons from cell death at 2 weeks after avulsion, whereas the NMDA receptor antagonists, MK-801 and D-AP5, had no effect on motor neuron survival (Figs. 6 and 7).

DISCUSSION

In the present study we have demonstrated that after avulsion injury of the L4 and L5 nerve roots the corresponding motoneurons in the spinal cord showed a marked reduction in immunoreactivity for the GluR2 subunit, whereas GluR1 and GluR4 labeling remained unchanged, suggesting that the reduction in GluR2 expression was not an epiphenomenon caused by the injured motoneurons. Furthermore, this decrease preceded motoneuron death in the L4 and L5 spinal cord segments. We found that in normal controls, motor neurons expressed GluR2 at relatively high levels, with the other AMPA receptor subunits and the NR1 subunit at various levels. The